

# Constraining Majorana CP phase in precision era of cosmology and double beta decay experiment

Hisakazu Minakata<sup>1,2,\*</sup>, Hiroshi Nunokawa<sup>1,\*</sup>, and Alexander A. Quiroga<sup>1,\*</sup>

<sup>1</sup> *Departamento de Física, Pontifícia Universidade Católica do Rio de Janeiro, C. P. 38071, 22452-970, Rio de Janeiro, Brazil*

<sup>2</sup> *Instituto de Física, Universidade de São Paulo, C. P. 66.318, 05315-970 São Paulo, Brazil*

\* *E-mail: hisakazu.minakata@gmail.com, nunokawa@puc-rio.br, alarquis@fis.puc-rio.br*

.....  
 We show that precision measurement of (1) sum of neutrino masses by cosmological observation and (2) lifetime of neutrinoless double beta decay in ton-scale experiments, with supplementary use of (3) effective mass measured in single beta decay experiment, would allow us to obtain information on the Majorana phase of neutrinos. To quantify the sensitivity to the phase we use the CP exclusion fraction, a fraction of the CP phase parameter space that can be excluded for a given set of assumed input parameters, a global measure for CP violation. We illustrate the sensitivity under varying assumptions, from modest to optimistic ones, on experimental errors and theoretical uncertainty of nuclear matrix elements. Assuming that the latter can be reduced to a factor of  $\simeq 1.5$  we find that one of the two Majorana phases (denoted as  $\alpha_{21}$ ) can be constrained by excluding  $\simeq 10 - 40\%$  of the phase space at  $2\sigma$  CL even with the modest choice of experimental error for the lowest neutrino mass of 0.1 eV. The characteristic features of the sensitivity to  $\alpha_{21}$ , such as dependences on the true values of  $\alpha_{21}$ , are addressed.  
 .....

Subject Index      B52, B54, C04, C43, F23

## 1. Introduction

After all the angles in the lepton mixing matrix [1] and the mass squared differences of neutrinos are determined by the atmospheric, the solar, the reactor, as well as the accelerator neutrino oscillation experiments, we have entered into a new phase of neutrino physics [2–4]. Of course, we are still with the important unknowns in the lepton sector, CP violating phase of the Kobayashi-Maskawa type [5] and the neutrino mass ordering. Yet, we do have relatively clearer view of how these questions are to be settled, either through the ongoing searches, or by new measurement to be carried out by the powerful apparatus described in various experimental proposals to date.

It is quite possible that even after these unknown quantities are measured by experiments the questions of somewhat different category will still remain: What are the absolute masses of neutrinos? Are neutrinos Dirac or Majorana particles? If Majorana, which values of the Majorana CP phases [6–8] are chosen by nature? The first one, knowing the absolute mass scale, is crucial to understand physics behind the origin of neutrino mass, and the latter two are likely the key to understand baryon number asymmetry in the universe [9].

In this paper, we focus on detectability of the Majorana CP phase in the light of informations to be obtained by cosmological observation and neutrino experiments in the coming

---

precision era. In particular, in the near future the double beta decay experiments aim to cover entire region of parameters allowed by the inverted mass ordering,<sup>1</sup> see Fig. 1. We show that given the future perspective, when combined with precision measurement in cosmology, one can indeed expect some sensitivities, though limited ones, to one of the phases (denoted as  $\alpha_{21}$ , see section 2.1). We hope that this result can trigger renewed interests in the problem of detectability of the Majorana phase despite the dominant pessimism which prevailed in the past decades. See, e.g., Refs. [10–21] for the foregoing efforts which examined the sensitivity to the Majorana phase.

We feel that the present moment is the particularly right time to revisit these issues because of the following reasons. Firstly, cosmological observations entered into the precision era so that their data became sensitive to the absolute masses of neutrinos better than the current bounds from laboratory experiments, as seen most notably by the results obtained by the Planck collaboration [22]. See also Ref. [23] for overview and many relevant references. It makes us possible to employ a new strategy that the absolute neutrino mass scale can be constrained mainly by cosmology and we can use data of neutrinoless double beta decay experiments, with supplementary use of single beta decay data, to constrain the Majorana phases of neutrinos. Even more interestingly a discrepancy between the cosmic microwave background (CMB) and lensing observations about cluster correlations would prefer massive neutrinos with mass of a few tenth of eV [24]. If confirmed, it would make the basis of our analysis more robust.

Secondly, as mentioned above, several new neutrinoless double beta decay experiments are in line to measure or constrain, the “ee” element of neutrino mass matrix in the flavor basis, so called the effective Majorana mass, to a few tens of meV [25–33]. For reviews and description of the other projects, see e.g., Refs. [34–36]. Needless to say, they are the prime candidates among various experiments that can measure or constrain the Majorana phases. We should also note that intensive efforts have been devoted in order to improve the calculations of the nuclear matrix element (NME) which is crucial to determine the value of effective Majorana mass from the measured half life time in double beta decay experiments [37–47]. See, also Ref. [36] for review of the recent progress in the calculations of NME.

Thirdly, the uncertainties in the relevant lepton mixing angles get decreased dramatically recently. The error of  $\sin^2 \theta_{12}$  is now only  $\sim 4\%$ [48], and moreover it will be decreased to a sub-percent level by the future medium-baseline reactor experiments [49, 50]. The mixing angle  $\theta_{13}$  whose value was unknown until recently before intriguing indication from T2K [51] by  $\nu_e$  appearance events, is now precisely measured [52, 53]. The error of  $\sin^2 \theta_{13}$  will soon reach to a even greater precision,  $\sim 5\%$  level. See Fig. 1 which shows how small is the effect of the current uncertainties of the mixing parameters onto the allowed regions by double beta decay experiments. These developments are important to tighten up the constraint on Majorana CP phases and to place it on a firmer ground.

In addition, the single beta decay experiment KATRIN [54] (see also [55]) will constrain neutrino masses to a level of 0.2 eV at 90 % CL, or observe the effects consistent with masses of this order, in a manner quite complementary to cosmological observations. While enjoying

---

<sup>1</sup> Throughout the paper the “ordering” of masses refers to that of the ones relevant for atmospheric neutrino oscillation, namely, normal (inverted) mass ordering corresponds to  $m_2 < m_3$  ( $m_2 > m_3$ ).

the above new inputs, our analysis is nothing but a continuation of the numerous similar analyses attempted by the many authors, from which we are certainly benefited.

To display the sensitivities to the Majorana CP phases in a global way, we use in this paper the CP exclusion fraction  $f_{\text{CPX}}$  [56], which is defined as a fraction of the CP phase space that can be excluded at a certain CL for a given set of input parameters. We believe that it is a useful tool particularly in the initial era of search for effects of the Majorana CP phase, in which even the partial exclusion of allowed range of the phase would be very valuable.<sup>2</sup> In [56]  $f_{\text{CPX}}$  was used to display sensitivity to the lepton Kobayashi-Maskawa phase achievable in the ongoing long-baseline neutrino oscillation experiments. For earlier discussion of a CP sensitivity measure closely related to  $f_{\text{CPX}}$  see [57, 58].

In the following two sections, 2 and 3, we briefly review the basic features of the observables used and describe simple analytic estimation of the effects of Majorana phases. The expert readers must go directly to the analysis results given in sections 5 and 6, starting from describing the analysis method in section 4.

## 2. Assumptions and observables used in the analysis

In this work we assume that the neutrinos are Majorana particles, and their Majorana masses are the unique source of neutrinoless double beta decay. We also assume the standard three-flavor mixing scheme of neutrinos.

In our analysis we consider the following three observables [59]:

- (1) the effective neutrino mass measured by neutrinoless double beta (hereafter denoted as  $0\nu\beta\beta$ ) decay experiment

$$\begin{aligned} m_{0\nu\beta\beta} &= \left| m_1 |U_{e1}|^2 + m_2 |U_{e2}|^2 e^{i\alpha_{21}} + m_3 |U_{e3}|^2 e^{i\alpha_{31}} \right| \\ &= \left| m_1 c_{13}^2 c_{12}^2 + m_2 c_{13}^2 s_{12}^2 e^{i\alpha_{21}} + m_3 s_{13}^2 e^{i\alpha_{31}} \right|, \end{aligned} \quad (1)$$

- (2) the sum of the three neutrino masses which can be determined by cosmological observation

$$\Sigma \equiv m_1 + m_2 + m_3, \quad (2)$$

- (3) the effective neutrino mass measured by single beta decay experiment

$$m_\beta = [m_1^2 c_{13}^2 c_{12}^2 + m_2^2 c_{13}^2 s_{12}^2 + m_3^2 s_{13}^2]^{\frac{1}{2}}, \quad (3)$$

where  $m_i$  ( $i = 1, 2, 3$ ) are neutrino masses and  $U_{ek}$  ( $k = 1, 2, 3$ ) are the element of electron-row of the Maki-Nakagawa-Sakata (MNS) neutrino mixing matrix [1]. We use its standard parameterization with notations  $c_{ij} \equiv \cos \theta_{ij}$ ,  $s_{ij} \equiv \sin \theta_{ij}$  [60], whereas  $\alpha_{21}$  and  $\alpha_{31}$  denote the Majorana CP phases, in which we have redefined  $\alpha_{31} - 2\delta$  in Eq. (14.82) in [60] as  $\alpha_{31}$  for simplicity.

All the three observables above are sensitive to masses of neutrinos, but they display different dependences on the mixing parameters, which makes them complementary to each

---

<sup>2</sup>On the other hand,  $f_{\text{CPX}}$  has intimate connection to the error of CP phase, an appropriate measure in precision measurement era, as discussed in [56]. It suggests that the CP exclusion fraction can be a universally usable measure for CP sensitivity.

other to detect the absolute mass scale. From the viewpoint of exploring the Majorana phase,  $m_{0\nu\beta\beta}$  and the other two play different roles under the assumed errors taken in our analysis. Of course, the information on Majorana phase is contained only in  $m_{0\nu\beta\beta}$ , but the constraint on the absolute mass scale from the other two is indispensable to produce sensitivity to the phase, as we will see clearly in section 5. The latter two are also complementary to each other. Cosmological measurement of  $\Sigma$ , though it may achieve greater accuracy in the future, relies on the assumption that we understand the rest of the universe. On the other hand, no such assumption is necessary for beta decay measurement in the laboratories as far as they can reach the neutrino mass scale given by nature.

In the rest of this section, after briefly mentioning their current status, we discuss some relevant issues on them in relationship to our analysis in this paper.

### 2.1. Current status and issues in neutrinoless double beta decay

The rate of  $0\nu\beta\beta$  decay, or the inverse of the half life time  $T_{1/2}^{0\nu}$  of the  $0\nu\beta\beta$  decay, is related to the effective neutrino mass  $m_{0\nu\beta\beta}$  in (1) as

$$[T_{1/2}^{0\nu}]^{-1} = G_{0\nu} \left| \mathcal{M}^{(0\nu)} \right|^2 \left( \frac{m_{0\nu\beta\beta}}{m_e} \right)^2, \quad (4)$$

where  $m_e$  is the electron mass,  $G_{0\nu}$  is the kinematic phase space factor, which can be calculated very accurately [61, 62], while  $\mathcal{M}^{(0\nu)}$  is the nuclear matrix element (NME) corresponding to the  $0\nu\beta\beta$  transition which is largely uncertain.

The next generation  $0\nu\beta\beta$  decay search aims at reaching the region of  $m_{0\nu\beta\beta}$  to  $\sim 10$  meV, which cover the entire inverted mass ordering branch. (See Fig. 1.) Toward approaching to the goal, the ongoing experiments are improving the lower bound of  $0\nu\beta\beta$  decay lifetime. Using  $^{76}\text{Ge}$  nuclei GERDA obtained the limit  $T_{1/2}^{0\nu} > 2.1 \times 10^{25}$  years at 90% CL, which is translated into the upper bound on  $m_{0\nu\beta\beta}$  of the range 0.2 – 0.4 eV depending upon the NME used [25]. KamLAND-Zen [26] and EXO-200 [27], both using  $^{136}\text{Xe}$ , derived the bound on lifetime  $T_{1/2}^{0\nu} > 1.9 \times 10^{25}$  (90% CL) and  $T_{1/2}^{0\nu} > 1.1 \times 10^{25}$  (90% CL) years, respectively. The latter bound becomes less stringent than the previously reported one from EXO-200 [28] because they found 9.9 events consistent with the  $0\nu\beta\beta$  decay signal. A joint analysis of KamLAND-Zen and the previous EXO-200 results are carried out by the KamLAND-Zen group who obtained a bound  $T_{1/2}^{0\nu} > 3.4 \times 10^{25}$  (90% CL) [26]. It corresponds to the upper limit of the effective mass  $m_{0\nu\beta\beta} < 0.1 - 0.25$  eV (90% CL).

The largest uncertainty in translating the bounds on  $T_{1/2}^{0\nu}$  to that of  $m_{0\nu\beta\beta}$  comes from the uncertainty of the NME,  $\mathcal{M}^{(0\nu)}$ . Currently, it produces differences of a factor of  $\sim 2 - 4$  on  $m_{0\nu\beta\beta}$  for a given measured lifetime  $T_{1/2}^{0\nu}$ . Despite that extensive efforts have been devoted to this issue, there are still considerable differences among NME values obtained by different authors and by different calculation methods. Generally speaking, the difference between different authors is not very large if the same calculation technique is used. The best hope would be to normalize the coupling strength by using the  $2\nu$  decay by which the difference may go down to  $\simeq 30\%$  level, as proposed within the framework of quasi-particle random phase approximation (QRPA) method [37, 38]. But, notable difference persists to among

---

results calculated by different techniques.<sup>3</sup> We expect that once the positive signal of  $0\nu\beta\beta$  will be observed by using different isotopes, by comparing the real data from these different isotopes, it would be possible to check the validity of various theoretical calculations based on different models or methods in a systematic way, which should allow to reduce significantly the NME uncertainty. For this reason we consider uncertainty on the NME a factor of less than or equal to 2 in this paper.

Recently, it was pointed out that renormalization effect on the axial vector coupling constant in the nuclear medium can have a sizable impact on the relationship between  $m_{0\nu\beta\beta}$  and half life [46]. It is likely that it affects the analysis which aims at detecting the effects of the Majorana phase such as ours in an  $A$ -dependent manner, and it is important to discuss influence of the effect. Unfortunately, we cannot address this issue in this paper because of the simplicity of our  $\chi^2$  construction.

## 2.2. Cosmological observation of sum of neutrino masses

The recent high precision cosmological observation became sensitive to the sum of the neutrino masses  $\Sigma$  defined in (2). With baryon acoustic oscillation (BAO) data the Planck collaboration obtained their most stringent limit  $\Sigma < 0.23$  eV (Planck + WMAP + highL + BAO) at 95% CL [22]. The authors of Ref. [63] obtained a stronger bound,  $\Sigma < 0.18$  eV at 95% CL, by adding the large-scale matter power spectrum data from the WiggleZ Dark Energy Survey [64].

More recently, some analyses started to favor non-zero best fit value of  $\Sigma$  [24, 65, 66] of active or sterile neutrinos. There exists some tension between strength of cluster correlations determined by CMB and the lensing observations within the Planck data itself as well as including other data sets. One of the ways to reduce the tension is to introduce neutrino masses. The authors of [24], assuming the active neutrinos, obtained the best fit value  $\Sigma = 0.32 \pm 0.081$  eV, which implies that  $m_1 \sim m_2 \sim m_3 \sim 0.1$  eV in the three flavour scheme. We expect that the issue is to be resolved in future cosmological observation; The data either from galaxy surveys or weak lensing by the Euclid satellite, with Planck constraints, may lead to the sensitivity to  $\Sigma \simeq 0.01 - 0.05$  eV [67–70].

Despite the progress in tightening up the neutrino mass bound by cosmological observation and the great precision expected in the future, we should keep in mind that the analysis has done and needs to be done within a particular cosmological model. Since neutrinos plays relatively minor role in determining the CMB spectrum and affecting the structure formation, we suspect that precision measurement of  $\Sigma$  requires a well established framework describing our universe and its time evolution.<sup>4</sup> Therefore, as a prerequisite of our analysis in this paper, we assume that the *standard model (SM) of cosmology* is established at the time one can execute precision measurement of half-life of  $0\nu\beta\beta$  decay. It would not be the

---

<sup>3</sup> It appears that the QRPA method [41–43] and the interacting boson model [44, 46] systematically lead to larger NME values than that calculated by the interacting shell model [40, 47]. See e.g., Table I and Fig. 1 of Ref. [45] in which a comparison between the NME values obtained by these models is made.

<sup>4</sup> The minor role played by neutrinos in the cosmos is indicated, for example, by the fact that the best fit to the current cosmological data does not require presence of neutrino masses, as reported in [71].

too optimistic to assume it because now already precise cosmological data by the Planck and the other observations are well described by the  $\Lambda$ CDM model (see Sec. 2.2).

### 2.3. Measurement of energy spectrum near the end point in single beta decay

The absolute neutrino mass scale can be probed by laboratory experiment which measures in a high precision electron energy spectrum at the end point in single beta decay [72]. The effective neutrino mass  $m_\beta$  measured by this method can be written as in (3). Currently, the best upper bound on  $m_\beta$  comes from Mainz [73] and Troitsk [74] experiments which place the upper bound  $m_\beta < 2.3$  eV and  $m_\beta < 2.05$  eV, respectively, both at 95% CL.

In the near future, we expect that the bound will be improved by an order of magnitude by the KATRIN experiment [54] which is expected to reach the sensitivity of  $m_\beta \sim 0.2$  eV at 90% CL. If the neutrino mass pattern is indeed the almost degenerate type, as suggested by some analyses of recent cosmological data [24, 65, 66], KATRIN has a chance of executing first model-independent determination of the absolute neutrino mass, and at the same time also serves for cross checking the cosmological measurement.

## 3. Analytic estimate of the effect of Majorana phase

In this section, we discuss qualitative features of effects of the Majorana phase onto the  $0\nu\beta\beta$  decay observable  $m_{0\nu\beta\beta}$ , aiming at illuminating how and where the best sensitivity to the Majorana phase can be expected. See also the discussions in the references cited in Sec. 1, as well as, e.g., in Refs. [75–78]. After presenting a familiar (and informative) plot of  $m_{0\nu\beta\beta}$  as a function of  $m_0$  [79], the lowest neutrino mass, we start by mentioning a general properties of  $m_{0\nu\beta\beta}$ .

### 3.1. Allowed regions of $m_{0\nu\beta\beta}$ as a function of lightest neutrino mass

In this paper we use the lightest neutrino mass (rather than  $\Sigma$ ), denoted as  $m_0$ , as the relevant parameter (observable) to be determined by the experiments. Namely,  $m_0 \equiv m_1$  and  $m_0 \equiv m_3$  for the normal and the inverted mass orderings, respectively. All the other masses and their differences can be calculated by using the relations

$$m_1 \equiv m_0, \quad m_2 = \sqrt{m_0^2 + \Delta m_{21}^2}, \quad m_3 = \sqrt{m_0^2 + \Delta m_{21}^2 + \Delta m_{32}^2} \quad (\text{normal mass ordering}), \quad (5)$$

$$m_1 = \sqrt{m_0^2 - \Delta m_{21}^2 - \Delta m_{32}^2}, \quad m_2 = \sqrt{m_0^2 - \Delta m_{32}^2}, \quad m_3 \equiv m_0 \quad (\text{inverted mass ordering}), \quad (6)$$

In Fig. 1, we show the allowed region of  $m_{0\nu\beta\beta}$  as a function of  $m_0$  for both the normal and the inverted mass orderings. The allowed region is calculated by the two ways, without and with the current  $1\sigma$  uncertainties of the mixing parameters, which are indicated, respectively, by the dark and light colors, with the blue and green colors for the inverted and normal mass ordering. It is remarkable that the effect of  $1\sigma$  uncertainties of the mixing parameters is quite small by now. In contrast, variation over the Majorana phases  $\alpha_{21}$  and  $\alpha_{31}$  gives much larger impact on allowed region of  $m_{0\nu\beta\beta}$ , not only producing sizeable width but also creating a down-going branch in region  $10^{-3}$  eV  $\lesssim m_0 \lesssim 10^{-2}$  eV for the case of the normal mass ordering due to the strong cancellation of the three mass terms in Eq. (1).

The difference between the normal and the inverted mass ordering becomes clearly visible only in small  $m_0$  region, typically  $m_0 \lesssim 0.1$ eV. Therefore, onset to the almost degenerate

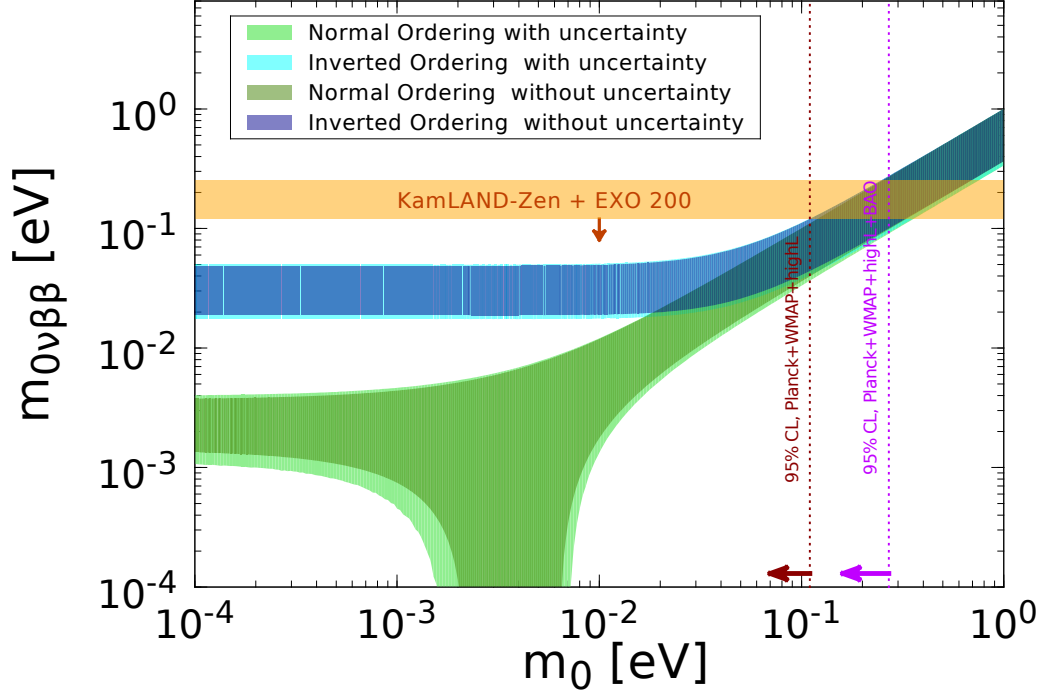


**Fig. 1** The currently allowed ranges of  $m_{0\nu\beta\beta}$  observables of  $0\nu\beta\beta$  decay is shown as a function of the lightest neutrino mass  $m_0$ . In the case of normal (inverted) mass ordering the ranges are shown by green (blue) colour. The light (dark) coloured regions are computed by taking into account (without taking account) the current  $1\sigma$  uncertainties of the relevant mixing parameters. Also shown are the limits on  $m_{0\nu\beta\beta}$  coming from KamLAND-Zen and EXO [26] (by the light brown band and arrow), the bounds on  $m_0$  obtained by Planck collaboration [22] (by the magenta and the brown dotted lines). We note that the KamLAND-EXO bound spans a band (not line) because of the NME uncertainty.

mass regime, which is formally defined as  $m_0 \gg \sqrt{\Delta m_{\text{atm}}^2} \simeq 0.05$  eV, already takes place for  $m_{0\nu\beta\beta}$  and  $m_\beta$  at around  $m_0 \gtrsim 0.1$  eV.

In Fig. 1 and in the rest of this paper we use the values obtained in [80]:

$$\begin{aligned} \Delta m_{21}^2 &= 7.54 \times 10^{-5} \text{ eV}^2, \\ \sin^2 \theta_{12} &= 0.308 \text{ or } \sin^2 2\theta_{12} = 0.853, \end{aligned} \quad (7)$$

for the both mass orderings whereas

$$\begin{aligned} \Delta m_{32}^2 &= 2.40 \text{ } (-2.44) \times 10^{-3} \text{ eV}^2, \\ \sin^2 \theta_{13} &= 0.0234 \text{ } (0.0239) \text{ or } \sin^2 2\theta_{13} = 0.0914 \text{ } (0.0933), \end{aligned} \quad (8)$$

for the normal (inverted) mass ordering.<sup>5</sup> Using these values of the parameters  $m_{0\nu\beta\beta}$  at its current status can be summarized as

$$m_{0\nu\beta\beta} \simeq |0.676 \text{ } (0.675) m_1 + 0.301 m_2 e^{i\alpha_{21}} + 0.0234 \text{ } (0.0239) m_3 e^{i\alpha_{31}}| \quad (9)$$

<sup>5</sup> Since the best fitted values of mass squared difference for atmospheric neutrino oscillation,  $\Delta m^2$ , shown in Table I of Ref. [80], is defined as  $\Delta m^2 \equiv m_3^2 - (m_1^2 + m_2^2)/2$ , the values of  $\Delta m_{32}^2$  in Eq. (8) were obtained by using the relation  $\Delta m_{32}^2 = \Delta m^2 - \Delta m_{21}^2/2$ .

for the normal (inverted) mass ordering.

### 3.2. Reduction of Majorana phase space

We describe here a general properties of  $m_{0\nu\beta\beta}$  given in (1). Since the phases  $\alpha_{21}$  and  $\alpha_{31}$  enter into  $m_{0\nu\beta\beta}$  in the form of either one of  $\cos \alpha_{21}$ ,  $\cos \alpha_{31}$ , and  $\cos(\alpha_{31} - \alpha_{21})$   $m_{0\nu\beta\beta}$  has the following reflection symmetry

$$m_{0\nu\beta\beta}(m_0, \alpha_{21}, \alpha_{31}) = m_{0\nu\beta\beta}(m_0, 2\pi - \alpha_{21}, 2\pi - \alpha_{31}). \quad (10)$$

Notice that it is an invariance under the simultaneous transformation of two phase variables  $\alpha_{21}$  and  $\alpha_{31}$ , and each one of them alone does not keep  $m_{0\nu\beta\beta}$  invariant.

### 3.3. The case of almost degenerate mass spectra

The best place to discuss clearly how and where the best sensitivity to the Majorana phase can be expected is in the almost degenerate regime,  $m_1 \approx m_2 \approx m_3$ , as ensured if  $m_0 \gg \sqrt{\Delta m_{\text{atm}}^2} \simeq 0.05$  eV, where  $\Delta m_{\text{atm}}^2 \equiv |\Delta m_{32}^2|$ . Moreover, the regime turns out to be the main target of our analysis, given reasonable values of experimental errors in the next generation  $0\nu\beta\beta$  decay experiments. In this regime, the effective mass  $m_{0\nu\beta\beta}$  in (1) can be written approximately to leading order in  $s_{13}^2$  as

$$m_{0\nu\beta\beta} \simeq c_{13}^2 m_0 \times \left[ 1 - \sin^2 2\theta_{12} \sin^2 \left( \frac{\alpha_{21}}{2} \right) + \frac{1}{2} \sin^2 2\theta_{13} \{ c_{12}^2 \cos \alpha_{31} + s_{12}^2 \cos(\alpha_{21} - \alpha_{31}) \} \right]^{\frac{1}{2}} \quad (11)$$

for the both mass orderings. The dominant effect of the Majorana phase is induced by  $\alpha_{21}$  because the last term in the square bracket in (11) has a  $\theta_{13}$  suppression and is smaller by a factor of 10 – 20 than the other terms. Ignoring the  $\sin^2 2\theta_{13}$  term, the maximum and minimum values of  $m_{0\nu\beta\beta}$  (upper and lower edges of the bands for  $m_0 \gtrsim 0.1$  eV in the plot in Fig. 1) are simply given, respectively, by

$$m_{0\nu\beta\beta}^{\text{max}} \simeq c_{13}^2 m_0, \quad m_{0\nu\beta\beta}^{\text{min}} \simeq c_{13}^2 m_0 \cos 2\theta_{12} \simeq 0.383 m_{0\nu\beta\beta}^{\text{max}}. \quad (12)$$

It means that the ratio of the maximum to the minimum value of effective mass changes by a factor of  $m_{0\nu\beta\beta}^{\text{max}}/m_{0\nu\beta\beta}^{\text{min}} \simeq 2.6$  as the Majorana phase is varied. Therefore, if one can determine  $m_{0\nu\beta\beta}$  from experiment with errors smaller than the factor 2.6, after taking into account the uncertainty coming from the NME, it is in principle possible to constrain the Majorana phase  $\alpha_{21}$ .

Since the sensitivity to the Majorana phase arises in places where the NME uncertainty cannot obscure the effect of phases, the best place is at the maximal and the minimal value of  $m_{0\nu\beta\beta}$ . One can show that the best sensitivity to  $\alpha_{21}$  is obtained at either  $\alpha_{31} = 0$  or  $\pi$ .<sup>6</sup> On the contrary, the worst sensitivity is expected at around the mean value of  $m_{0\nu\beta\beta}$  between their maximum and minimum values. Typically, they are at around  $\alpha_{21} \simeq 2\pi/3$  for the whole range of  $\alpha_{31}$ . These features will be confirmed explicitly by quantitative analysis in section 6.

<sup>6</sup>  $m_{0\nu\beta\beta}$  in (11) is nearly periodic function of  $\alpha_{21}$  and  $\alpha_{31}$ , and has the following properties in regions  $0 \leq \alpha \leq \pi$ : (1) The function inside parenthesis in Eq. (11) is an extremely slowly decreasing function of  $\alpha_{31}$  for in the entire region of  $\alpha_{21}$ . (2) It is a decreasing function of  $\alpha_{21}$  in the entire region of  $\alpha_{31}$ , and varies from  $\simeq 1$  to  $\simeq 0.15$  as  $\alpha_{21}$  is varied from 0 to  $\pi$ . Therefore, it has the maximum (minimum) at  $\alpha_{21} = \alpha_{31} = 0$  ( $\alpha_{21} = \alpha_{31} = \pi$ ).

### 3.4. Hierarchical case; inverted mass spectrum

Now let us consider the case of  $m_0 < \sqrt{\Delta m_{21}^2} \lesssim 0.01$  eV for the inverted mass ordering. In this case,  $m_1 \approx m_2 \sim \sqrt{\Delta m_{\text{atm}}^2} \gg m_3 \equiv m_0$ . This is the regime corresponding to the horizontal band for the inverted mass spectra in Fig. 1. It is interesting to observe that essentially the same treatment can go through for  $m_{0\nu\beta\beta}$  as in the case of almost degenerate spectrum. In the case of strongly hierarchical inverted mass spectrum the  $m_3$  term in (9) is doubly suppressed than other two terms by a factor of  $m_3/m_2 \ll [\Delta m_{21}^2/\Delta m_{\text{atm}}^2]^{1/2} \simeq 0.18$  and  $s_{13}^2 = 0.0234$  (0.0239) for the normal (inverted) ordering. In the case of almost degenerate spectrum the suppression of  $m_3$  term is only due to the latter factor. Under the approximation of ignoring the  $m_3$  term,  $m_{0\nu\beta\beta}$  is expressed as in the degenerate case, (11) without  $s_{13}^2$  term, but replacing  $m_0$  by  $\sqrt{\Delta m_{\text{atm}}^2}$ ,

$$m_{0\nu\beta\beta} \simeq c_{13}^2 \sqrt{\Delta m_{\text{atm}}^2} \left[ 1 - \sin^2 2\theta_{12} \sin^2 \left( \frac{\alpha_{21}}{2} \right) \right]^{\frac{1}{2}}. \quad (13)$$

Since the dependence of  $m_{0\nu\beta\beta}$  on the Majorana phase is essentially the same as in the case of the degenerate mass regime, the same results hold for the sensitivity to  $\alpha_{21}$  and the location of highest sensitivity. Under our assumption of the precision of measurement,  $\sigma_{0\nu\beta\beta} (\equiv \text{error of } m_{0\nu\beta\beta}) = 0.01$  eV (see section 4), however, the sensitivity to  $\alpha_{21}$  is quite limited in this regime when it is combined with the NME uncertainty. It will be demonstrated in the analysis in section 6.

### 3.5. Hierarchical case; normal mass spectrum

If  $m_0 \ll \sqrt{\Delta m_{21}^2}$ , typically  $m_0 \sim 10^{-4}$  eV, one can ignore  $m_1 (= m_0)$  term in Eq. (9). Then, we obtain the expression of  $m_{0\nu\beta\beta}$  as

$$\begin{aligned} m_{0\nu\beta\beta} &= \sqrt{\Delta m_{21}^2} \left[ s_{12}^4 c_{13}^4 + 2 \sqrt{\frac{s_{13}^4}{\epsilon}} s_{12}^2 c_{13}^2 \cos(\alpha_{31} - \alpha_{21}) \right]^{1/2} \\ &\simeq \sqrt{\Delta m_{21}^2} [0.0905 + 0.0794 \cos(\alpha_{31} - \alpha_{21})]^{1/2} \end{aligned} \quad (14)$$

where  $\epsilon \equiv \Delta m_{21}^2/\Delta m_{\text{atm}}^2 \simeq 0.0314$  and we have kept order  $\sqrt{s_{13}^4/\epsilon}$  term which is  $\simeq 0.13$ , but ignored the terms of order  $\epsilon^2$ ,  $s_{13}^4$ ,  $s_{13}^4/\epsilon \simeq 5.3 \times 10^{-4}/0.0314 \simeq 0.017$  and  $\sqrt{\epsilon} s_{13}^2 \simeq 4.1 \times 10^{-3}$ . Thus, in the normal mass ordering with small  $m_0$  region, the phase  $\alpha_{31}$  (in a combination  $\alpha_{31} - \alpha_{21}$ ) affects the  $0\nu\beta\beta$  decay rate, in contrast to the case of almost degenerate and inverted mass spectra in which only  $\alpha_{21}$  plays a role. As  $\alpha_{31}$  changes  $m_{0\nu\beta\beta}$  varies as

$$\sqrt{\Delta m_{21}^2} \left[ s_{12}^4 c_{13}^4 - 2 \sqrt{\frac{s_{13}^4}{\epsilon}} s_{12}^2 c_{13}^2 \right]^{1/2} \leq m_{0\nu\beta\beta} \leq \sqrt{\Delta m_{21}^2} \left[ s_{12}^4 c_{13}^4 + 2 \sqrt{\frac{s_{13}^4}{\epsilon}} s_{12}^2 c_{13}^2 \right]^{1/2}. \quad (15)$$

Or numerically,

$$0.105 \sqrt{\Delta m_{21}^2} \simeq 9.12 \times 10^{-4} \text{ eV} \leq m_{0\nu\beta\beta} \leq 0.412 \sqrt{\Delta m_{21}^2} \simeq 3.58 \times 10^{-3} \text{ eV} \quad (16)$$

a factor of  $\sim 4$  variation. Again, under our assumption of the precision of  $\sigma_{0\nu\beta\beta} = 0.01$  eV it would be very difficult to probe the value of  $\alpha_{31}$  in this regime, as we will see in section 6.

---

## 4. Analysis Method

### 4.1. Assumptions on experimental errors

We use the three observables, sum of neutrino masses  $\Sigma$ , which is determined by cosmology, and the effective mass parameters  $m_\beta$  and  $m_{0\nu\beta\beta}$  which are measured, respectively, by single and double beta decay experiments. Let us assume that they are measured with some uncertainties around the central values,  $m_{0\nu\beta\beta}^{(0)}$ ,  $\Sigma^{(0)}$ , and  $m_\beta^{(0)}$ :

$$m_{0\nu\beta\beta}^{\text{obs}} = m_{0\nu\beta\beta}^{(0)} \pm \sigma_{0\nu\beta\beta}, \quad (17)$$

$$\Sigma^{\text{obs}} = \Sigma^{(0)} \pm \sigma_\Sigma, \quad (18)$$

$$m_\beta^{\text{obs}} = m_\beta^{(0)} \pm \sigma_\beta, \quad (19)$$

where  $\sigma_{0\nu\beta\beta}$ ,  $\sigma_\Sigma$ , and  $\sigma_\beta$  denote the corresponding  $1\sigma$  uncertainties. Due to the uncertainty in the NME calculations, one must pay special attention to the precise meaning of  $m_{0\nu\beta\beta}^{(0)}$ . See the next subsection regarding this point. We take the following values for the uncertainties,

$$\sigma_{0\nu\beta\beta} = 0.01 \text{ eV}, \quad \sigma_\Sigma = 0.05 \text{ eV}, \quad \sigma_\beta = 0.06 \text{ eV}, \quad (20)$$

which will be used as the reference values in our analysis.

Here is some reasonings for our choices of the uncertainties in (20). To have a reasonable estimate of the uncertainty in  $m_{0\nu\beta\beta}$ , we need a detailed discussion because we must address the question of how the experimental uncertainty on  $T_{1/2}^{0\nu}$  is translated into that of  $m_{0\nu\beta\beta}$ , and the treatment heavily depend on to what extent the experimental backgrounds can be suppressed. We present such a discussion in Appendix A, based on the earlier treatment e.g., in Refs. [36, 81]. Under the assumption of dominance of statistical error, we will argue there that the uncertainty of 0.01 eV may be reachable in future experiments that are upgraded to a ton scale. Such experiments will be able to cover the entire allowed range corresponding to the inverted mass ordering, and the similar region of  $m_{0\nu\beta\beta}$  in the normal mass ordering.

As is mentioned in Sec. 2.2, we assume that the SM of cosmology will be established by the time the  $0\nu\beta\beta$  decay experiments reach the above accuracy. Because of the success of the  $\Lambda$ CDM model to explain the current data sets it is likely that the SM of cosmology is not too far away from the  $\Lambda$ CDM model. Then, we may be allowed to use the value of the uncertainty in  $\Sigma$  estimated within the current framework of  $\Lambda$ CDM model. It is expected that the future galaxy surveys [67] and weak lensing [68] both lead, under the Planck constraint, the sensitivity to  $\Sigma$  to the level of 0.02 – 0.05 eV. According to the authors of Ref. [70], in the most optimistic case, the sensitivity could even lead to  $\sim 0.01$  eV. Therefore, our reference error on  $\Sigma$  would be in a conservative side, and the alternative choice  $\sigma_\Sigma = 0.02$  eV which we will also examine would not be too optimistic in view of [70].

For KATRIN [55] they quote the error  $0.025 \text{ eV}^2$  for  $m_\beta^2$ , which may be translated into the error of 0.063 eV for  $m_\beta$  for the case where true value of  $m_0 = 0.2$  eV, which justifies our choice in (20).

### 4.2. Analysis procedure: $\chi^2$ and treatment of NME errors

As we emphasized in section 2.1 the error of  $m_{0\nu\beta\beta}$  due to uncertainties of the NME would be a major obstacle to extract informations of the Majorana phases from  $0\nu\beta\beta$  decay experiments. We take into account the uncertainties of NME via the following way,

which is very similar to the one proposed in [19] but with different functional form. Let us assume that the unknown true value of NME, which we denote as  $\mathcal{M}^{(0\nu)}$ , exists in a range  $\mathcal{M}_{\min}^{(0\nu)} \leq \mathcal{M}^{(0\nu)} \leq \mathcal{M}_{\max}^{(0\nu)}$ . Practically,  $\mathcal{M}_{\min}^{(0\nu)}$  and  $\mathcal{M}_{\max}^{(0\nu)}$  imply, respectively, the minimum and the maximum values of NME calculated in a consistent framework. We may define the NME uncertainty factor as  $r_{\text{NME}} \equiv \mathcal{M}_{\max}^{(0\nu)} / \mathcal{M}_{\min}^{(0\nu)}$ . Then, if we define  $\xi$  as

$$\xi \equiv \frac{\mathcal{M}_{\text{av}}^{(0\nu)}}{\mathcal{M}^{(0\nu)}} \quad (21)$$

where  $\mathcal{M}_{\text{av}}^{(0\nu)} \equiv \left( \mathcal{M}_{\max}^{(0\nu)} \mathcal{M}_{\min}^{(0\nu)} \right)^{1/2}$ ,  $\xi$  falls into a region  $1/\sqrt{r_{\text{NME}}} \leq \xi \leq \sqrt{r_{\text{NME}}}$ . We note that our  $\xi$  corresponds to inverse of  $\xi$  defined in [19].

In this work, we consider the three values of the NME uncertainty parameter,  $r_{\text{NME}} = 1.3, 1.5$  and  $2.0$ . (Exceptional use of an extreme value,  $r_{\text{NME}} = 1.1$ , is made at the end of section 6.) We note that, strictly speaking, errors associated with the three observables we consider in this work would not be Gaussian, in particular, the one from cosmology. It should be better to do analysis based on Monte Carlo simulations, as performed, e.g., in Refs. [82, 83]. However, we believe that the procedure we use produces approximately correct results, which are sufficient for our purpose.

Using the three observables in (17) - (19), we define the  $\chi^2$  function as follows,

$$\chi^2 \equiv \min \left\{ \left[ \frac{\Sigma^{(0)} - \Sigma^{\text{fit}}(m_0)}{\sigma_\Sigma} \right]^2 + \left[ \frac{m_\beta^{(0)} - m_\beta^{\text{fit}}(m_0)}{\sigma_\beta} \right]^2 + \left[ \frac{\xi m_{0\nu\beta\beta}^{(0)} - m_{0\nu\beta\beta}^{\text{fit}}(m_0, \alpha_{21}, \alpha_{31})}{\sigma_{0\nu\beta\beta}} \right]^2 \right\}, \quad (22)$$

where  $\Sigma^{(0)}$ ,  $m_\beta^{(0)}$  and  $m_{0\nu\beta\beta}^{(0)}$  are the central values to be determined by the future experiments whereas  $\Sigma^{\text{fit}}(m_0)$ ,  $m_\beta^{\text{fit}}(m_0)$  and  $m_{0\nu\beta\beta}^{\text{fit}}(m_0, \alpha_{21}, \alpha_{31})$  are the ones to be fitted by varying the parameters  $m_0$ ,  $\alpha_{21}$  and  $\alpha_{31}$ . We also vary the parameter  $\xi$  in the interval of  $[1/\sqrt{r_{\text{NME}}}, \sqrt{r_{\text{NME}}}]$  by taking flat prior assuming no preference among the estimated values of NME. In this way, the NME uncertainty is treated in a similar way as the flux ratio parameter in the solar neutrino analysis to determine the true neutrino flux in comparison to the calculated flux by the Standard Solar Model, as was done, e.g., in Ref. [84].

To summarize, we minimize the  $\chi^2$  by varying  $m_0$ ,  $\alpha_{21}$ ,  $\alpha_{31}$  and  $\xi$ , and determine the allowed parameter space by imposing the condition,

$$\Delta\chi^2 \equiv \chi^2 - \chi_{\min}^2 < 2.3, 6.18 \text{ and } 11.83 \quad (1, 4 \text{ and } 9) \quad (23)$$

for 1, 2 and  $3\sigma$  CL for two (one) degrees of freedom.

Throughout this paper we use the mixing parameters described in (7) and (8). We do not consider the uncertainties of the mixing parameters apart from the currently unknown mass ordering, because the impact is rather small which is expected to become even smaller in the near future. This is because we expect significant improvement in the accuracies of these parameters by future oscillation experiments, in particular, by the medium baseline ( $\sim 50 - 60$  km) reactor experiments such as JUNO [49] and RENO-50 [50] as demonstrated, e.g., in Refs. [85-88].

## 5. Sensitivity to the Majorana Phase: Why so much constraint?

In this section, we have a glance over the global features of sensitivity to the Majorana phase, and try to understand the reasons why such nontrivial constraint on the phase arises despite that a large uncertainty exists in calculating the NME.

### 5.1. Allowed regions of $m_0$ , $\alpha_{21}$ and $\alpha_{31}$

Let us consider the case where the true values of relevant fundamental parameters are,  $m_0 = 0.1$  ( $\Sigma \simeq 0.32$  eV) and  $\alpha_{21} = \alpha_{31} = \pi$ . In Fig. 2 the allowed regions projected into the planes of (a)  $\alpha_{21} - m_0$  (b)  $\alpha_{21} - \alpha_{31}$  and (c)  $m_0 - \alpha_{31}$  are drawn. The NME uncertainty is taken as  $r_{\text{NME}} = 1.5$ . In the case of inverted mass ordering they are depicted by the filled colours, yellow, red, and light blue, corresponding, respectively, to 1, 2 and 3 $\sigma$  CL for 2 degree of freedom (DOF). While for the normal mass ordering they are drawn by the black dotted (1 $\sigma$ ), dashed (2 $\sigma$ ) and the solid (3 $\sigma$ ) curves.

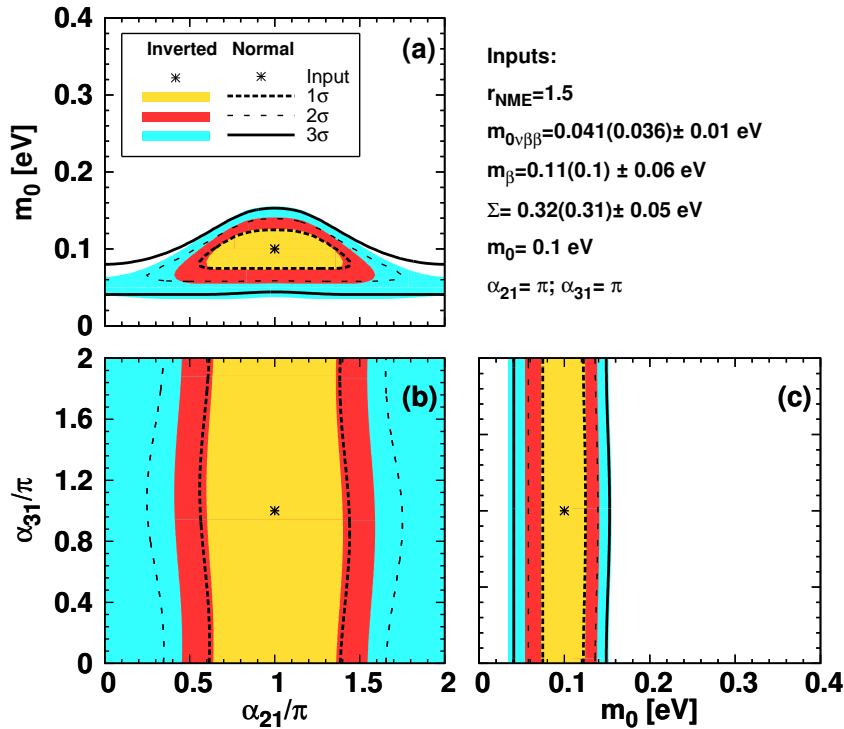


**Fig. 2** Regions allowed at 1, 2 and 3 $\sigma$  CL indicated by the filled color of yellow, red and light blue, respectively, for 2 DOF, projected into the planes of (a)  $\alpha_{21} - m_0$  (b)  $\alpha_{21} - \alpha_{31}$  and (c)  $m_0 - \alpha_{31}$  for the case of the inverted mass ordering and the true values of  $m_0 = 0.1$  eV,  $\alpha_{21} = \alpha_{31} = \pi$ , and  $r_{\text{NME}} = 1.5$ . The allowed contours of the normal mass ordering are shown by the dotted (1 $\sigma$ ), dashed (2 $\sigma$ ), and solid (3 $\sigma$ ) curves. In the legend, the numbers outside (inside) the parentheses corresponds to the inverted (normal) mass ordering.

We notice from Fig. 2 that it is possible to restrict  $\alpha_{21}$  in some interval at 2 $\sigma$  CL for 2 DOF, but not at 3 $\sigma$  CL, the feature which is valid for the both mass orderings. On the other hand, it is not possible to constrain at all the phase  $\alpha_{31}$ , as it can be expected by the smallness of the third term proportional to  $m_3$  in (1) due to  $\theta_{13}$  suppression. We have checked that this is true for any values of  $\alpha_{31}$  because the dependence of the allowed regions on  $\alpha_{31}$  is always very mild. We also note that the allowed regions in Fig. 2(b) are symmetric with respect to  $\alpha_{21} = \pi$  in a good approximation. It stems from the simultaneous reflection symmetry  $\alpha_{21} \rightarrow 2\pi - \alpha_{21}$  and  $\alpha_{31} \rightarrow 2\pi - \alpha_{31}$  in Eq. (10) and the weak dependence of  $\Delta\chi^2$  on  $\alpha_{31}$ .

If we repeat the same exercise with  $m_0 = 0.2$  eV ( $\Sigma \simeq 0.61$  eV), the  $3\sigma$  allowed region of  $\alpha_{21}$  is restricted to  $0.5\pi \lesssim \alpha_{21} \lesssim 1.5\pi$ . The difference between the normal and inverted mass orderings, which is visible at  $m_0 \simeq 0.1$  eV (Fig. 2), diminishes at  $m_0 \gtrsim 0.2$  eV. The difference is evident at  $m_0 \lesssim 0.05$  eV (not shown here, but see [89]), where the sensitivity to  $\alpha_{21}$  still persists in the case of inverted ordering, as seen in (13). Since the dependence on  $\alpha_{31}$  is quite mild, from now on we will show only the allowed regions projected onto the plane of  $\alpha_{21} - m_0$ , which is the most interesting combination for our purpose.

### 5.2. Why and how does constraint on the Majorana phases arise?

One may ask why such nontrivial constraints on  $\alpha_{21}$  arise despite the presence of NME uncertainty  $\xi$  in (22). To give the readers a feeling we focus on the case of almost degenerate mass spectrum discussed in section 3.3. In this case  $m_{0\nu\beta\beta}$  determined by nature is related to the “observed” one, the inferred one with use of particular NME as  $m_{0\nu\beta\beta}^{\text{obs}} = \xi^{-1}m_{0\nu\beta\beta}^{\text{true}}$ , where  $m_{0\nu\beta\beta}^{\text{true}}$  is given by (11). Since  $m_{0\nu\beta\beta}^{\text{obs}} \propto \xi^{-1}m_0$ , if we are completely ignorant about  $m_0$ , there is no way to constrain the value of  $\alpha_{21}$  even in the case of no NME uncertainty ( $\xi = 1$ ) no matter how accurately  $m_{0\nu\beta\beta}$  itself is determined. Therefore, the first requirement for a sensitivity to the Majorana phases is to have an independent measurement of absolute neutrino mass scale other than  $0\nu\beta\beta$  decay.<sup>7</sup> The second requirement is that the uncertainty of NME is not too large. We note that the variation of  $m_{0\nu\beta\beta}^{\text{true}}$  is as large as a factor of  $\simeq 2.6$  as  $\alpha_{21}$  is varied from 0 to  $2\pi$ . (see section 3.3). Then,  $\alpha_{21}$  can be constrained only if the NME uncertainty cannot compensate the variation.

Let us now examine in more detail how non-vanishing  $\Delta\chi^2$  develops to produce the constraint on  $\alpha_{21}$ . In Fig. 3 the contributions to  $\Delta\chi^2$  from the three types of experiments are plotted as a function of  $\alpha_{21}$  for the case of inverted mass ordering. The dotted blue, dashed green, and the solid red curves indicate, in order,  $\Delta\chi^2$  obtained when only  $0\nu\beta\beta$  decay experiment is considered, when the  $\beta$  decay data is added, and all the three experiments are considered (i.e., the cosmological measurement of  $\Sigma$  is also added). As it stands, the single beta and  $0\nu\beta\beta$  decay experiments cannot constrain the value of  $\alpha_{21}$  at CL higher than  $1\sigma$ . We confirmed that this feature is true even if there is no NME uncertainty. But, once the cosmological observation of  $\Sigma$  is added,  $\Delta\chi^2$  jumps in region outside  $0.6\pi - 1.4\pi$  of  $\alpha_{21}$ , as shown by the solid red curve in Fig. 3. We, however, stress that the relative strength of the experiments in constraining  $\alpha_{21}$  heavily relies on our error estimates in (20). If we repeat the similar exercise as in Fig. 3 with the normal mass ordering, we observe that the sensitivity to the Majorana phase is lower. The shape of  $\Delta\chi^2$  is very similar to that of the inverted ordering, but the height is about  $2/3$  of the  $\Delta\chi^2$  curves in Fig. 3.<sup>8</sup>

Therefore, in region  $m_0 \gtrsim 0.1$  eV,  $0\nu\beta\beta$  decay experiments can produce nontrivial constraint on  $\alpha_{21}$  by circumventing the NME uncertainty, but only when it is combined with

<sup>7</sup>We note, however, that this is not always true for the case of non-degenerate neutrino mass spectrum, in particular in region  $m_0 \ll 0.1$  eV. In certain cases it would be possible to constrain the CP phase only using the information from  $0\nu\beta\beta$  decay experiment.

<sup>8</sup>It is because, for a given value of  $m_0$ , the first and second terms which contain  $m_1$  and  $m_2$ , respectively, in (1) are always larger in the case of inverted ordering than the ones in the normal one, as we can see from (5) and (6). Assuming the difference between  $|\Delta m_{32}^2|$  in both mass ordering is small, as is the case in (8), it makes  $\Delta\chi^2$  for the inverted mass ordering larger, thereby making the inverted mass ordering case more sensitive to the change of  $\alpha_{21}$ .

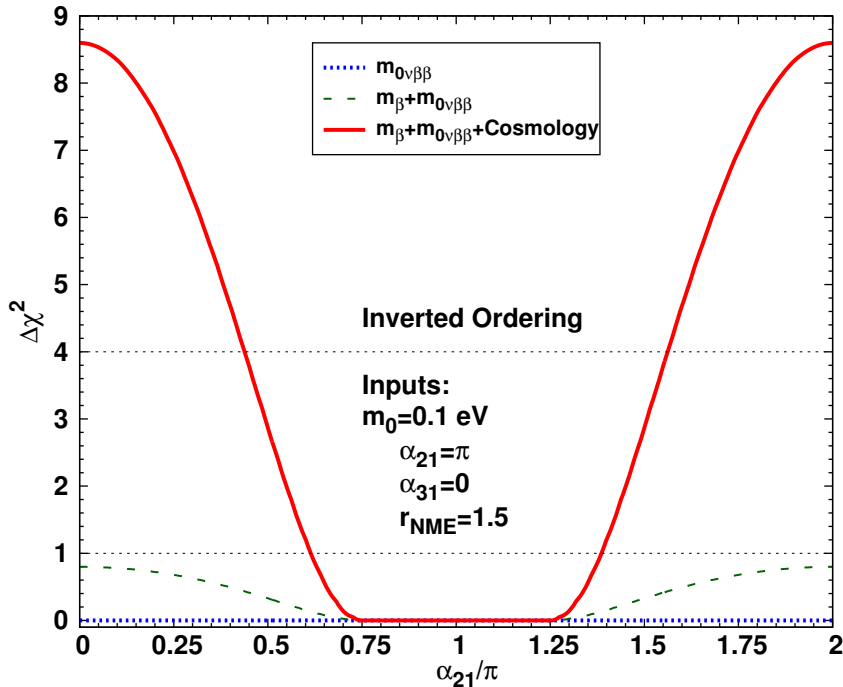


**Fig. 3**  $\Delta\chi^2$  is plotted as a function of the fitted value of  $\alpha_{21}$  for the case of the inverted mass ordering. The true values of the parameters are taken as  $m_0 = 0.1$  eV,  $\alpha_{21} = \pi$ , and  $\alpha_{31} = 0$ . The three  $\Delta\chi^2$  curves are presented which correspond to three combinations of the data used in the analysis, only  $0\nu\beta\beta$  decay (dotted blue line),  $0\nu\beta\beta + \beta$  decays (dashed green curve) and all combined,  $0\nu\beta\beta + \beta$  decays + cosmology (solid red curve). In the fit the remaining parameters,  $m_0$  and  $\alpha_{31}$ , are marginalized.

precision measurement of absolute mass scale of neutrinos. We note that at the bottom of  $\Delta\chi^2$  in the region where  $\alpha_{21} = 0.75\pi - 1.25\pi$ ,  $\chi_{\min}^2$  is very flat because of the NME uncertainty. It means that it is impossible to pin down, in the presence of the NME uncertainty, the value of the Majorana phase  $\alpha_{21}$  at the bottom no matter how accurately all the measurements are done.

In the case of inverted mass ordering with hierarchical spectrum,  $m_{0\nu\beta\beta}$  is given by (13), and the role of  $m_0$  in the above discussion is played by  $\sqrt{\Delta m_{\text{atm}}^2}$ . Therefore, an accurate measurement of  $\Delta m_{\text{atm}}^2$ , in principle, replaces the cosmological measurement. However,  $m_{0\nu\beta\beta}$  is small,  $m_{0\nu\beta\beta} \sim 0.05$  eV, in this region, and the error taken in (20) is relatively large. Then, we do not expect significant sensitivity to the Majorana phase. This last statement applies also to the normal mass ordering with hierarchical spectrum. These features as well as the ones discussed above for the degenerate mass spectrum will be demonstrated in the next section.

## 6. Analysis results: Sensitivity to the Majorana phase

In this section, we show the results of our analysis on sensitivity to the Majorana phase  $\alpha_{21}$  by using the CP exclusion fraction  $f_{\text{CPX}}$  [56]. It is defined as the fraction of values of  $\alpha_{21} \in [0, 2\pi]$  which can be excluded by the experiments at a given confidence level for each input

point of the parameter space  $(m_0, \alpha_{21})$  and a given NME uncertainty. It is a global measure for CP sensitivity and may be particularly useful in the initial stage in which the sensitivity to the CP phase may be limited. For more about  $f_{\text{CPX}}$  see Ref. [56].

### 6.1. CP exclusion fraction: the case of reference errors

We show in the three rows in Fig. 4 the results obtained for the CP exclusion fraction  $f_{\text{CPX}}$ , which indicates that some sensitivities to the Majorana phase do indeed exist. (1) First row: shown are the iso-contours of the CP exclusion fraction determined at  $2\sigma$  (95.45%) CL (1 DOF) in the plane spanned by the true values of  $\alpha_{21}$  and the lightest neutrino mass  $m_0$ . Both  $\alpha_{21}$  and  $m_0$  are varied in the fit. (2) Second row:  $f_{\text{CPX}}$  is plotted as a function of the true values of  $\alpha_{21}$  at  $m_0 = 0.1$  and  $0.3$  eV where input value of  $m_0$  is fixed but it is varied in the fit. Roughly speaking, it is nothing but the cross section of the iso-contours of  $f_{\text{CPX}}$  at the values of  $m_0$ . (3) Third row:  $f_{\text{CPX}}$  as a function of true values of  $m_0$  at  $\alpha_{21} = 0, \pi/2$ , and  $\pi$ . Similar to the case of (2), input value of  $\alpha_{21}$  is fixed but it is varied in the fit.<sup>9</sup> In each row the left, middle and the right panels are for uncertainties of the NME,  $r_{\text{NME}} = 2.0, 1.5$ , and  $1.3$ , respectively. The second and third rows are provided for ease of understanding the complex structure of the iso-contours of  $f_{\text{CPX}}$  given in the first row. Due to the symmetry (10), the iso-contours of  $f_{\text{CPX}}$  are symmetric under reflection around  $\alpha_{21} = \pi$  after marginalizing over  $\alpha_{31}$ . Hence, we show the results only for the range of  $0 \leq \alpha_{21} \leq \pi$ . Notice that larger the values of  $f_{\text{CPX}}$ , higher the sensitivity to  $\alpha_{21}$  because larger fraction of the phase space can be excluded.

In the first row, the iso-contours of  $f_{\text{CPX}}$  for the inverted and the normal mass orderings are depicted, respectively, by the solid and the dashed lines, from 0.1 to 0.7 (with the step size of 0.1), using different colors as indicated in the legend. In the second and third rows the case of inverted (normal) mass ordering is depicted by using colored band (dotted, dashed, or dash-dotted lines). We note that for each point on the input parameter space, all the parameters,  $m_0, \alpha_{21}, \alpha_{31}$  and  $\xi$  were varied in doing the fit. In Fig. 4 the true value of  $\alpha_{31}$  is taken to be 0, and the similar contour plot with  $\alpha_{31} = \pi$  (not shown here, see [89]) indicates that the sensitivity is slightly higher but not much.<sup>10</sup>

As can be seen most clearly in the second row of Fig. 4, the sensitivity to  $\alpha_{21}$  is highest in region around  $\alpha_{21} \simeq \pi$  and next highest in region of  $\alpha_{21}$  near 0. The worst sensitivity is obtained at around  $\alpha_{21} \sim 2\pi/3$ , in agreement with the qualitative discussion given in section 3. Yet, it may be interesting to note that the sensitivity improves at around the worst sensitive region if the NME errors are controlled better, as can be seen in the middle and right panels (e) and (f) in Fig. 4. As expected the difference between the normal and the inverted mass orderings are small in the degenerate regime,  $m_0 \gtrsim 0.1$  eV where the colored bands (inverted) and dashed double dotted line (normal) in the second and third rows, overlap rather well. A better sensitivity to the phase  $\alpha_{21}$  for the inverted than the

<sup>9</sup> To obtain  $f_{\text{CPX}}$  plots in the second and third rows marginalization over the fitted parameters is carried out, which produces a finite width of the  $f_{\text{CPX}}$  curves.

<sup>10</sup> We have examined the similar  $f_{\text{CPX}}$  plots for several input values of  $\alpha_{31}$ ,  $0, \pi/4, \pi/2$ , and  $\pi$ . The exercise revealed that for  $\alpha_{21} \gtrsim 0.6\pi$ , the best and the worst sensitivities are obtained at  $\alpha_{31} = \pi$  and  $\alpha_{31} = 0$ , respectively, the cases used in Fig. 4. For  $\alpha_{21} \lesssim 0.6\pi$ , this behaviour become opposite, leading to the worst and best sensitivity at  $\alpha_{31} = \pi$  and  $\alpha_{31} = 0$ , respectively,

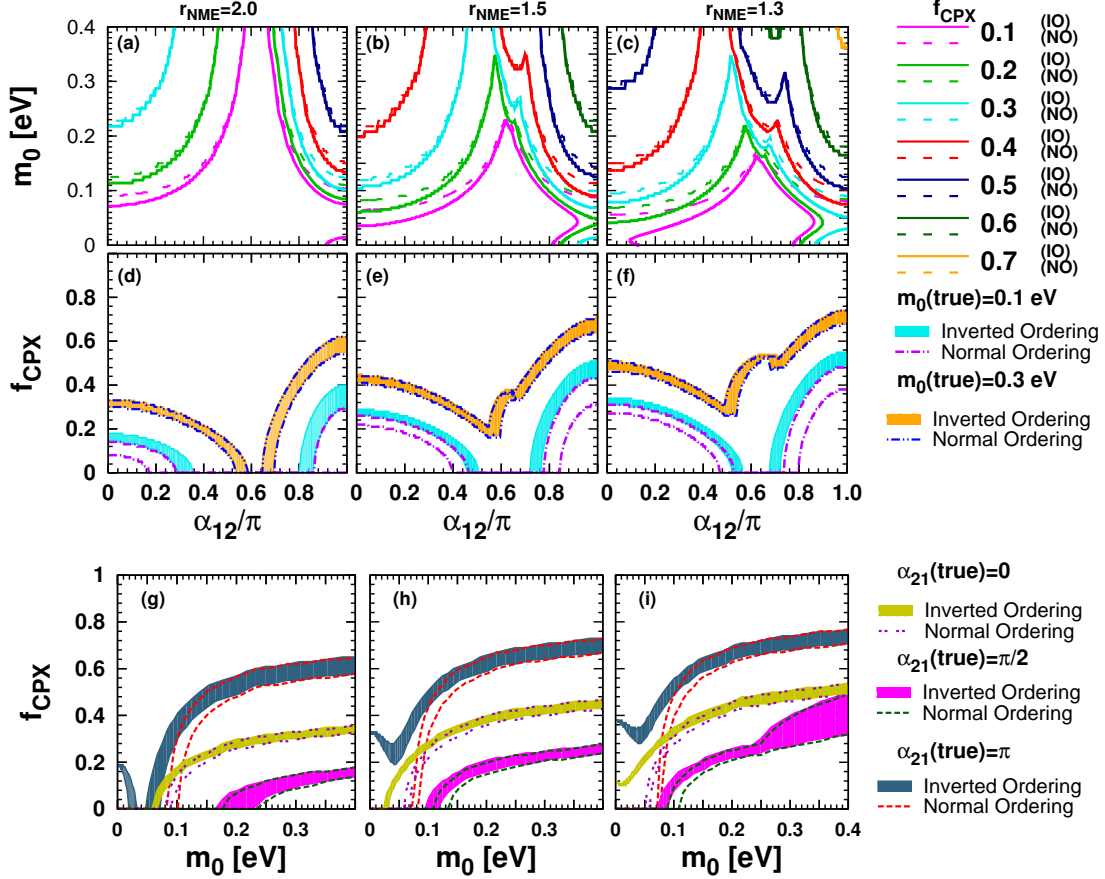


**Fig. 4** In the first row [panels (a), (b), and (c)]: shown are the iso-contours of the CP exclusion fraction determined at  $2\sigma$  (95.45%) CL (1 DOF) projected into the plane of the true values of  $\alpha_{21}/\pi$  and the lightest neutrino mass  $m_0$ . In the second row [panels (d), (e), and (f)]:  $f_{\text{CPX}}$  is plotted as a function of the true values of  $\alpha_{21}$  at  $m_0 = 0.1$  and  $0.3$  eV, which is nothing but slices of the iso-contours of  $f_{\text{CPX}}$  at the values of  $m_0$ . In the third row [panels (g), (h), and (i)]:  $f_{\text{CPX}}$  as a function of  $m_0$  at  $\alpha_{21} = 0, \pi/2$ , and  $\pi$ . In each row the left, middle and the right panels are for uncertainties of the NME  $r_{\text{NME}} = 2.0, 1.5$ , and  $1.3$ , respectively. The case for the inverted and normal mass orderings are shown, respectively, by the solid and dashed curves from 0.1 to 0.7 with the step size of 0.1 in the first row, and by using the colored band and dashed (dotted or dash-dotted) lines, respectively, in the remaining rows.

normal ordering case can be observed around region  $m_0 \sim 0.05$  eV where the sensitivity is however rather low.

It is important to notice that the sensitivity to  $\alpha_{21}$  strongly depends upon  $r_{\text{NME}}$ . In particular the improvement of the sensitivity from  $r_{\text{NME}} = 2.0$  to  $r_{\text{NME}} = 1.5$  is remarkable. At  $m_0 = 0.15$  eV, for example, while  $f_{\text{CPX}} \geq 0.3$  region spans only  $\simeq 0.2$  of  $\alpha_{21}$  space for  $r_{\text{NME}} = 2.0$ , it jumps to  $\simeq 50\%$  coverage for  $r_{\text{NME}} = 1.5$  for both cases of  $\alpha_{31} = 0$  and  $\pi$ . It is also notable that in the inverted mass ordering case the sensitivity region reaches to the

range  $0 \text{ eV} \leq m_0 \lesssim 0.05 \text{ eV}$ , though only up to  $f_{\text{CPX}} \simeq 0.1 - 0.2$ .<sup>11</sup> The tendency is more and more visible for smaller values of  $r_{\text{NME}}$ . Therefore, reducing the NME uncertainty is of crucial importance to have severer constrains on (or to observe) the Majorana phase.

### 6.2. CP exclusion fraction: the case of more optimistic errors

Though it is encouraging to see some sensitivities to the Majorana phase thanks to precision measurement of  $\Sigma$  and  $0\nu\beta\beta$  decay rate, we must remark that the sensitivity is still at a relatively low level. For example, in the case of  $m_0 \simeq 0.1 \text{ eV}$ , which is preferred by some cosmological analyses, the sensitivity to  $\alpha_{21}$  is up to the level of  $f_{\text{CPX}} \simeq 0.1 - 0.3$  even in the most optimistic case of  $r_{\text{NME}} = 1.3$  except for the region close to  $\alpha_{21} = \pi$  (see the second row of Fig. 4). Moreover, there always exists a region of  $\alpha_{21}$  in which  $f_{\text{CPX}}$  vanishes at around the worst sensitive region, and the region is quite wide for  $r_{\text{NME}} = 2.0$ .

Therefore, we examine below two possibilities toward further improvement of the sensitivity to  $\alpha_{21}$ : (1) Higher precision measurement of neutrino masses in cosmology as good as  $\sigma_\Sigma = 0.02 \text{ eV}$ , and (2) Revolutionary new technology of computing the NME of  $0\nu\beta\beta$  decay which could lead to uncertainty of the level  $r_{\text{NME}} = 1.1$ . As mentioned before, once the positive signal of  $0\nu\beta\beta$  will be observed by using different isotopes, we hope that theoretical NME calculations can be “calibrated” to some extent using the real data. (Nonetheless, we tentatively assume that 10% level uncertainty is unavoidable.) It is discussed that the former is within reach in the light of future cosmological observation as mentioned in section 2.2 [67–69]. On the other hand, it remains to be seen how (2) can be realized.

In Fig. 5 we present the results of  $f_{\text{CPX}}$  for these more optimistic experimental and theoretical uncertainties. In the upper and the lower clusters of six panels of Fig. 5, we show  $f_{\text{CPX}}$  as a function of the true value of  $\alpha_{21}$  at  $m_0 = 0.1$  and  $0.3 \text{ eV}$ , and  $f_{\text{CPX}}$  as a function of the true value of  $m_0$  at  $\alpha_{21} = 0, \pi/2$ , and  $\pi$ , respectively. In each cluster of panels the upper (lower) three panels are for cases with  $\sigma_\Sigma$  (the error of  $\Sigma$ ) of  $0.05 \text{ eV}$  ( $0.02 \text{ eV}$ ). The panels (a) and (b) both in the upper and the lower clusters in Fig. 5 are identical to the panels (e) and (f) in Fig. 4; They are duplicated to make comparison with the corresponding cases with the smaller uncertainties in the lower panels easier.

We observe that, globally, the sensitivity increases from left to right ( $r_{\text{NME}} = 1.5, 1.3, 1.1$ ), and from the upper to lower panels ( $\sigma_\Sigma = 0.05, 0.02 \text{ eV}$ ). However, the improvement in the sensitivity to the phase is relatively modest despite the highly nontrivial requirement on the uncertainties of  $r_{\text{NME}}$  or  $\sigma_\Sigma$ . Most notable exception may be that  $f_{\text{CPX}} \neq 0$  at  $m_0 = 0.1 \text{ eV}$  is realized for the first time within our analysis, which however, occurs for an extreme case of  $r_{\text{NME}} = 1.1$  and  $\sigma_\Sigma = 0.02 \text{ eV}$ . There exists significant variation in the sensitivity to the phase as the true value of  $\alpha_{21}$  is varied (lower cluster of panels). The similar dependence is also visible for varying  $m_0$  (upper cluster of panels). A good news is that at  $m_0 = 0.1 \text{ eV}$ , the average value of  $f_{\text{CPX}}$  reaches  $\simeq 0.3$  for the case  $\sigma_\Sigma = 0.02 \text{ eV}$  as seen in the panel (e) in the upper cluster in Fig. 5. In all the panels in the lower cluster the difference of  $f_{\text{CPX}}$  curves between the inverted and the normal mass orderings are quite visible in region at  $m_0 \lesssim 0.1 \text{ eV}$ .

<sup>11</sup> We note here that we took a fixed error ( $0.01 \text{ eV}$ ) for  $m_{0\nu\beta\beta}$  based on the discussion given in Appendix A. If a percentage error for  $m_{0\nu\beta\beta}$  is to be assumed, the sensitivity to  $\alpha_{21}$  in region  $m_0 \lesssim 0.05 \text{ eV}$  would be greatly enhanced.

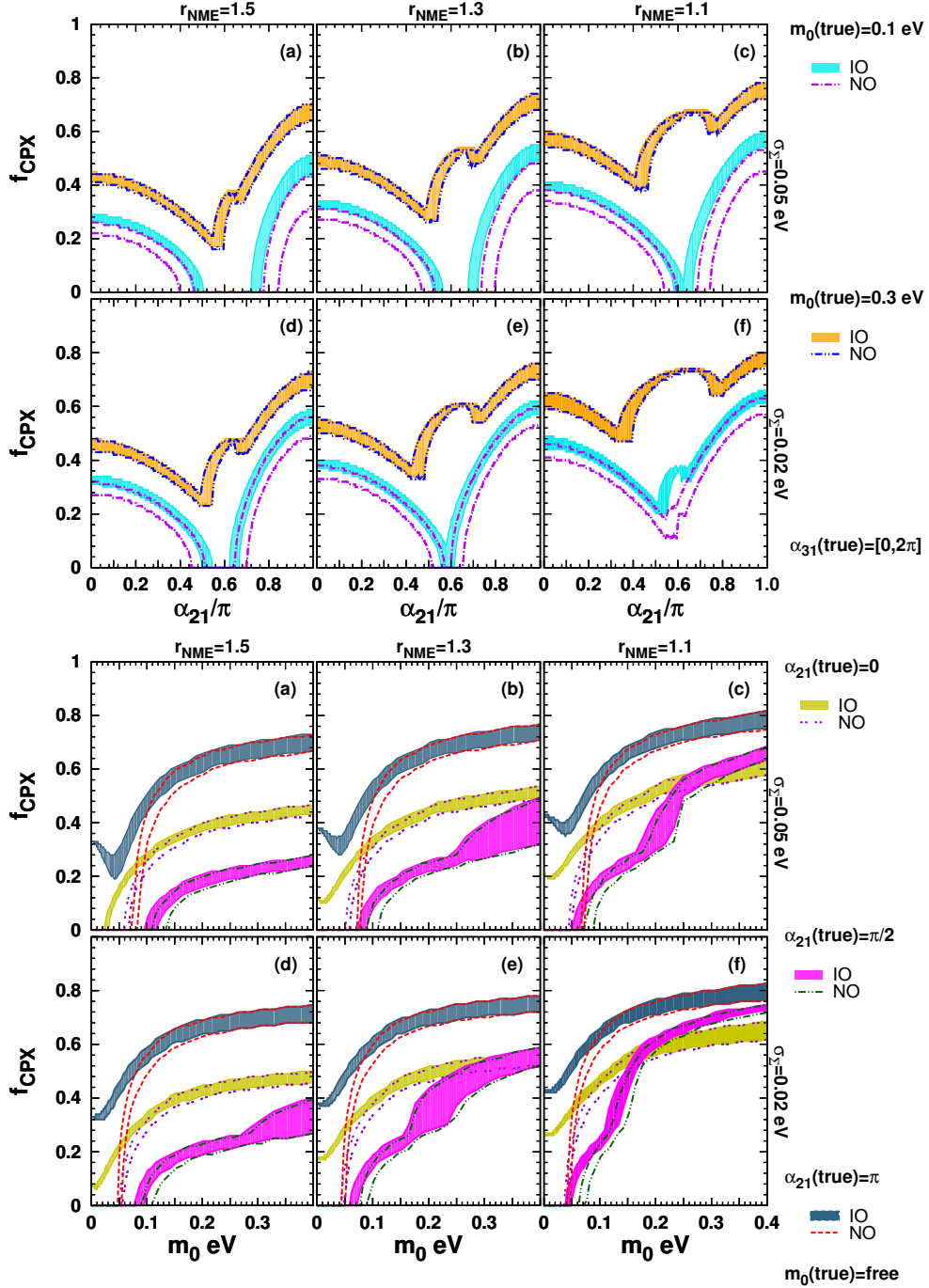


**Fig. 5** In the upper and the lower clusters of six panels, shown are  $f_{\text{CPX}}$  as a function of the true value of  $\alpha_{21}$  at  $m_0 = 0.1$  and  $0.3$  eV, and  $f_{\text{CPX}}$  as a function of the true value of  $m_0$  at  $\alpha_{21} = 0, \pi/2$ , and  $\pi$ , respectively. In both clusters the true value of  $(\sigma_\Sigma, r_{\text{NME}})$  used are: (a) (0.05 eV, 1.5), (b) (0.05 eV, 1.3), (c) (0.05 eV, 1.1), (d) (0.02 eV, 1.5), (e) (0.02 eV, 1.3), and (f) (0.02 eV, 1.1).

One may say that the sensitivity to  $\alpha_{21}$  is low, i.e., excluding only 30% of its phase space at  $2\sigma$  CL, which may be insufficient to foresee the measurement of the Majorana phase.

---

Nonetheless, we hope that the results we report in this paper would imply a nontrivial step to obtain perspectives for measuring the Majorana phase. Clearly, imaginative discussions on how to improve the sensitivity to the phase are called for.

## 7. Conclusions and discussion

Assuming the mass mechanism of  $0\nu\beta\beta$  decay, we have studied in this paper how and to what extent the Majorana phases can be constrained in the light of future accurate measurements of  $0\nu\beta\beta$  decay rate and an independent precision measurement of neutrino's absolute mass scale. In our estimates of the errors described in Sec. 4.1 cosmological observation of the sum of neutrino masses  $\Sigma$  plays the latter role. We have demonstrated that even in the situation that double beta decay experiment alone cannot say anything about the Majorana phase, it is possible to obtain highly non-trivial constraints on the Majorana phase, if accurate measurement of  $\Sigma$  is added. Indeed, it is unlikely that  $0\nu\beta\beta$  decay experiment by itself can place any useful constraints on the Majorana phase within our assumption of the experimental errors. Notice, however, that it is not because they suffer from the NME uncertainty (which of course makes the situation worse), but because they lack independent key information of the absolute neutrino mass scale in itself (see Sec. 5.2). The remarkable feature of our results is that the synergy between cosmology and double beta decay experiments in constraining the Majorana phase is quite visible.

The general tendency of the sensitivity to the Majorana phases are as follows:

- Dependence of  $m_{0\nu\beta\beta}$  on  $\alpha_{31}$ , one of the two Majorana phases, is very weak due to the suppression by  $s_{13}^2$ . Hence, little sensitivity can be expected for  $\alpha_{31}$ . The sensitivity to  $\alpha_{21}$  depend on  $\alpha_{31}$ , but only very weakly.
- The regions of the best and the worst sensitivities to  $\alpha_{21}$  are located at around the true values  $\alpha_{21} \simeq 0$  or  $\pi$ , and at  $\alpha_{21} \simeq 2\pi/3$ , respectively, in agreement with our analytic estimate in Sec. 3.3.
- For both mass orderings and within any uncertainties of the NME used, the better sensitivity to the CP phase  $\alpha_{21}$  is obtained for larger value of  $m_0$ , apart from minor exception of region  $m_0 \lesssim 0.05$  eV which is mostly in the horizontal branch in Fig. 1 for the inverted mass ordering.

We took as the reference set up of the uncertainties that the effective masses observed in  $0\nu\beta\beta$  and  $\beta$  decay experiments can be measured with the errors of 0.01 eV and 0.06 eV, respectively, whereas the sum of neutrino masses  $\Sigma$  can be determined with the uncertainty of 0.05 eV by cosmological observation. We have assumed the uncertainty factor  $r_{\text{NME}}$  (defined as the ratio of the maximum and minimum values of the theoretically expected NME values) of a range 1.3 – 2.0. We have treated it in a different way from these experimental errors, in similar way as the treatment of flux normalization uncertainty. To show the dependence of these assumed errors on sensitivity to Majorana phase, we have also examined the case with more optimistic errors, 0.02 eV for the error of  $\Sigma$  and  $r_{\text{NME}} = 1.1$  for the NME uncertainty.

To display the sensitivities to the Majorana phase globally we have used the new measures, the CP exclusion fraction,  $f_{\text{CPX}}$ , a fraction of the CP phase space that can be excluded for a given set of input parameters.  $f_{\text{CPX}}$  is a useful global measure, as the CP fraction widely used in the sensitivity studies for the long-baseline neutrino oscillation experiments is, but in a different way. We believe that  $f_{\text{CPX}}$  is better suited to reveal (relatively poor) sensitivities

---

in the early era of the search for the CP phase effect, as discussed in [56]. Since measuring the Majorana phase is very challenging in any means, we believe that even the partial exclusion of its possible range is quite useful.

We have shown with our reference setup and  $r_{\text{NME}} = 1.5$  that  $\alpha_{21}$  can be constrained by excluding  $\simeq 10 - 40\%$  of the phase space of  $\alpha_{21}$  at  $2\sigma$  CL for the lowest neutrino mass of 0.1 eV for both mass orderings. Even if we use 0.02 eV for the error of  $\Sigma$  the excluding fraction does not change much, and the exclusion fraction is  $\simeq 10 - 50\%$ . Fortunately, the  $f_{\text{CPX}}$  contours are rather stiff against change in confidence level from  $2\sigma$  to  $3\sigma$ , indicating robust nature of sensitivity to the Majorana phase. We also should note that the sensitivity to  $\alpha_{21}$  becomes significantly better when the uncertainty of the nuclear matrix element ( $r_{\text{NME}}$ ) is reduced from the factor 2 to 1.5, independent of the assumed mass ordering and value of  $\alpha_{31}$ .

It is only recently that such a discussion started to obtain real perspective because cosmology entered into the precision era, as demonstrated most notably by an epoch making precision measurement achieved by Planck. Yet, the accuracy of measurement of the sum of neutrino masses which warrants reasonably strong restriction to the Majorana phase is rather demanding,  $\sigma_{\Sigma} \simeq 0.02$  eV, which probably requires the Euclid satellite as well as the next generation galaxy surveys, in addition to the better understanding of the different systematics exist in the different set of the cosmological data. Of course, it also requires accurate measurement of lifetime of  $0\nu\beta\beta$  decay in a ton scale experiment with very low background, which would allow uncertainty in measurement of  $m_{0\nu\beta\beta}$  as small as  $\simeq 0.01$  eV.

One may argue that too much relying on cosmological observation in determining  $\Sigma$  is dangerous because, neutrinos being a minor player in the universe, its precise determination is possible only in a model dependent way. Though it is a valid point we must bear in mind that future precision observation itself offers an even more stringent test of the  $\Lambda$ CDM paradigm. Then, it may be conceivable that the SM of cosmology could be eventually born out from such process, which we assumed as a prerequisite of our analysis. It would allow us a reliable measurement of the neutrino component in the universe and to determine the sum of their masses with a sufficient robustness. The discussion in this paper would serve as a prototype of the similar analysis that should be done after we have acquired the established standard cosmological model.

### A. Estimation of the sensitivity to $m_{0\nu\beta\beta}$ in neutrinoless double beta decay experiment

Let us estimate the expected precision on  $m_{0\nu\beta\beta}$  to be observed in the  $0\nu\beta\beta$  decay experiment. See Refs. [34–36, 81, 90, 91] for more detailed discussions on the experimental sensitivities. Here we ignore the theoretical uncertainty of the nuclear matrix element,  $\mathcal{M}^{(0\nu)}$ , which will be taken care of in a different way as discussed in section 4.

From Eq. (4) we obtain the following expression for the effective mass,

$$m_{0\nu\beta\beta} = \frac{m_e}{\sqrt{T_{1/2}^{0\nu} G_{0\nu} |\mathcal{M}^{(0\nu)}|^2}}. \quad (\text{A1})$$

The expected number of  $0\nu\beta\beta$  decays (signal) to be observed in the experiment,  $N_{0\nu\beta\beta}$ , is given by

$$N_{0\nu\beta\beta} = \varepsilon_{\text{det}} \frac{m_X N_A}{W_X} \left[ 1 - \exp\left(-\frac{t_{\text{exp}} \ln 2}{T_{1/2}^{0\nu}}\right) \right] \simeq \frac{\varepsilon_{\text{det}} N_A m_X t_{\text{exp}} \ln 2}{W_X T_{1/2}^{0\nu}} \quad (\text{A2})$$

where  $\varepsilon_{\text{det}}$  is the detection efficiency,  $m_X$  and  $W_X$  are respectively, the total mass and the molecular weight of the isotope  $X$  to be used in the double beta decay experiment,  $N_A$  is the Avogadro's number and  $t_{\text{exp}}$  is the exposure time, assumed to be much smaller than  $T_{1/2}^{0\nu}$ .

On the other hand, the expected number of the background events can be expressed as,

$$N_{\text{BG}} = b \Delta E m_X t_{\text{exp}}, \quad (\text{A3})$$

where  $b$  is the number of background counts usually measured in  $\text{keV}^{-1} \cdot \text{kg}^{-1} \cdot \text{yr}^{-1}$ ,  $\Delta E$  is the energy window ( $\sim$  energy resolution) given in keV around the  $0\nu\beta\beta$  peak, both of which depend on the experimental set up we consider.

Roughly speaking, the expected sensitivity of the double beta decay experiment for the half life time is obtained when  $N_{0\nu\beta\beta} \sim \sqrt{N_{\text{BG}}}$ , which implies that

$$T_{1/2}^{0\nu} \sim \frac{\varepsilon_{\text{det}} N_A m_X t_{\text{exp}} \ln 2}{W_X \sqrt{b \Delta E m_X t_{\text{exp}}}} = \frac{\varepsilon_{\text{det}} N_A \ln 2}{W_X} \sqrt{\frac{m_X t_{\text{exp}}}{b \Delta E}}. \quad (\text{A4})$$

This can be translated in terms of the minimum possible observable value of  $m_{0\nu\beta\beta}^{\text{min}}$  as [92],

$$m_{0\nu\beta\beta}^{\text{min}} \sim \frac{m_e}{\sqrt{G_{0\nu} |\mathcal{M}(0\nu)|^2 \ln 2}} \left[ \frac{W_X}{\varepsilon_{\text{det}} N_A} \right]^{\frac{1}{2}} \left[ \frac{b \Delta E}{m_X t_{\text{exp}}} \right]^{\frac{1}{4}}. \quad (\text{A5})$$

If we consider, for example, the isotopes of  $^{76}\text{Ge}$  and  $^{136}\text{Xe}$ , by using the typical values for  $G_{0\nu}$  and  $\mathcal{M}(0\nu)$  found, e.g., in Ref. [36], and typical background rate and energy resolutions, for  $^{76}\text{Ge}$  (by using  $G_{0\nu} = 2.36 \times 10^{-15} \text{ yr}^{-1}$  [62]) we obtain,

$$m_{0\nu\beta\beta}^{\text{min}} \sim 0.12 \left[ \frac{5.0}{|\mathcal{M}(0\nu)|} \right] \left[ \frac{b}{0.01 \text{ keV}^{-1} \cdot \text{kg}^{-1} \cdot \text{yr}^{-1}} \right]^{\frac{1}{4}} \left[ \frac{\Delta E}{3.5 \text{ keV}} \right]^{\frac{1}{4}} \left[ \frac{100 \text{ kg} \cdot \text{yr}}{\varepsilon_{\text{det}}^2 \cdot m_{\text{Ge}} \cdot t_{\text{exp}}} \right]^{\frac{1}{4}} \text{ eV}, \quad (\text{A6})$$

whereas for  $^{136}\text{Xe}$  (by using  $G_{0\nu} = 14.58 \times 10^{-15} \text{ yr}^{-1}$  [62]) we obtain,

$$m_{0\nu\beta\beta}^{\text{min}} \sim 0.24 \left[ \frac{3.0}{|\mathcal{M}(0\nu)|} \right] \left[ \frac{b}{0.01 \text{ keV}^{-1} \cdot \text{kg}^{-1} \cdot \text{yr}^{-1}} \right]^{\frac{1}{4}} \left[ \frac{\Delta E}{100 \text{ keV}} \right]^{\frac{1}{4}} \left[ \frac{100 \text{ kg} \cdot \text{yr}}{\varepsilon_{\text{det}}^2 \cdot m_{\text{Xe}} \cdot t_{\text{exp}}} \right]^{\frac{1}{4}} \text{ eV}, \quad (\text{A7})$$

where  $m_{\text{Ge}}$  ( $m_{\text{Xe}}$ ) is the total mass of the isotope of  $^{76}\text{Ge}$  ( $^{136}\text{Xe}$ ) to be used in the double beta decay experiments. If  $0\nu\beta\beta$  decay will be actually observed, at first approximation, we assume that these values could be roughly corresponds to the uncertainty on the measurement of  $m_{0\nu\beta\beta}$ , or  $\sigma_{0\nu\beta\beta}$ .

As we can see, as the sensitivity improves only as the one of the fourth power of the size of the experiment, background and energy resolution, it is seems not so easy to improve the sensitivity and looks quite difficult to reach the level of  $\sigma_{0\nu\beta\beta} \sim O(0.01) \text{ eV}$ , even if we consider  $\sim 1$  ton scale experiment. Therefore, it would be necessary to realize the background free or very low background experiment to achieve such a level (see below).

Next let us consider the case that the background rate  $b$  is so low that  $N_{BG}$  in Eq. (A3) is negligible, or namely, *zero background* experiment [36]. In this case, from the number of observed events,  $N_{0\nu\beta\beta}$ , the half life time can be estimated as

$$T_{1/2}^{0\nu} = \frac{\varepsilon_{\text{det}} n_X t_{\text{exp}} \ln 2}{N_{0\nu\beta\beta}}, \quad (\text{A8})$$

and its uncertainty is estimated as

$$\delta(T_{1/2}^{0\nu}) \sim T_{1/2}^{0\nu} \frac{\delta(N_{0\nu\beta\beta})}{N_{0\nu\beta\beta}} \sim T_{1/2}^{0\nu} \frac{1}{\sqrt{N_{0\nu\beta\beta}}}. \quad (\text{A9})$$

Then from Eqs. (A1) and (A9) we obtain

$$\begin{aligned} \sigma_{0\nu\beta\beta} \equiv \delta(m_{0\nu\beta\beta}) &\sim \frac{1}{2} m_{0\nu\beta\beta}^{(0)} \frac{\delta(T_{1/2}^{0\nu})}{T_{1/2}^{0\nu}} \sim \frac{1}{2} m_{0\nu\beta\beta}^{(0)} \frac{1}{\sqrt{N_{0\nu\beta\beta}}} \\ &\sim \frac{m_e}{2\sqrt{G_{0\nu}} |\mathcal{M}^{(0\nu)}|^2 \varepsilon_{\text{det}} (m_X N_A / W_X) t_{\text{exp}} \ln 2}. \end{aligned} \quad (\text{A10})$$

We note that the result does not depend on the life time, and the uncertainty can be arbitrarily small as we increase the product of the source mass and exposure time of the experiment by considering only the statistical error, until the point that the background could no longer be neglected.

By using the same numbers for  $G_{0\nu}$  and  $\mathcal{M}^{(0\nu)}$  we used to obtain  $m_{0\nu\beta\beta}^{\text{min}}$  in Eqs. (A6) and (A7) and ), for  $^{76}\text{Ge}$ , we obtain,

$$\sigma_{0\nu\beta\beta} \sim 0.06 \left[ \frac{100 \text{ kg} \cdot \text{yr}}{\varepsilon_{\text{det}} \cdot m_{\text{Ge}} \cdot t_{\text{exp}}} \right]^{\frac{1}{2}} \left[ \frac{5.0}{\mathcal{M}^{(0\nu)}} \right] \text{ eV}, \quad (\text{A11})$$

whereas for  $^{136}\text{Xe}$ , we obtain,

$$\sigma_{0\nu\beta\beta} \sim 0.04 \left[ \frac{100 \text{ kg} \cdot \text{yr}}{\varepsilon_{\text{det}} \cdot m_{\text{Xe}} \cdot t_{\text{exp}}} \right]^{\frac{1}{2}} \left[ \frac{3.0}{\mathcal{M}^{(0\nu)}} \right] \text{ eV}. \quad (\text{A12})$$

We expect that these values should coincide roughly with the minimum possible observable values (or sensitivities) of the experiments, or  $\sigma_{0\nu\beta\beta} \sim m_{0\nu\beta\beta}^{\text{min}}$ . Therefore, as long as the background is neglected, by considering the  $\sim 1$  ton size experiment, it seems possible to reach the level of  $\sigma_{0\nu\beta\beta} \sim O(0.01)$  eV. In this work, for definiteness and simplicity, we assume that  $m_{0\nu\beta\beta}$  can be determined with an accuracy of 0.01 eV for a given reference value of the NME. See the section 4.2 how to take into account the NME uncertainty. We note, however, that in reality, the fate of the background would not be so simple to allow analytic treatment as ours. Therefore, most probably, one needs to perform detailed numerical simulations to reliably estimate the experimental uncertainties in measurement of the double beta decay lifetime.

## Acknowledgment

The authors thank Kunio Inoue for informative correspondences on neutrinoless double beta decay experiment and Shun Saito on the cosmological determination of neutrino masses. H.M. is grateful to CNPq for support for his visit to the Departamento de Física, Pontifícia Universidade Católica do Rio de Janeiro. He thanks Universidade de São Paulo for

the great opportunity of stay as Pesquisador Visitante Internacional. He is also partially supported by KAKENHI received through Tokyo Metropolitan University, Grant-in-Aid for Scientific Research No. 23540315, Japan Society for the Promotion of Science. H.N. thanks the hospitality of Osamu Yasuda and Omar Miranda, respectively, at the Department of Physics of Tokyo Metropolitan University and of CINVESTAV-IPN where the final part of this manuscript was done. This work was supported by Fundação de Amparo à Pesquisa do Estado do Rio de Janeiro (FAPERJ) and Conselho Nacional de Ciência e Tecnologia (CNPq).

### Note Added

After the first version of this paper [89] was submitted to arXiv, a preprint [93] appeared which addresses the constraint on the Majorana phase with the same framework of combining cosmological observations with  $0\nu\beta\beta$  decay experiments. It appears that a better sensitivity to the phase reported by them comes from the optimistic choice of uncertainties in  $0\nu\beta\beta$  decay measurement and in the NME,  $\sigma_{0\nu\beta\beta} = 0.01$  eV and  $r_{\text{NME}} = 1$ , if translated to our language.

### References

- [1] Z. Maki, M. Nakagawa and S. Sakata, *Prog. Theor. Phys.* **28**, 870 (1962).
- [2] T. Kajita, *Adv. High Energy Phys.* **2012**, 504715 (2012).
- [3] A. B. McDonald, *New J. Phys.* **6**, 121 (2004) [astro-ph/0406253].
- [4] K. Inoue, *New J. Phys.* **6**, 147 (2004).
- [5] M. Kobayashi and T. Maskawa, *Prog. Theor. Phys.* **49**, 652 (1973).
- [6] J. Schechter and J. W. F. Valle, *Phys. Rev. D* **22**, 2227 (1980).
- [7] S. M. Bilenky, J. Hosek and S. T. Petcov, *Phys. Lett. B* **94**, 495 (1980).
- [8] M. Doi, T. Kotani, H. Nishiura, K. Okuda and E. Takasugi, *Phys. Lett. B* **102**, 323 (1981).
- [9] M. Fukugita and T. Yanagida, *Phys. Lett. B* **174** 45, (1986).
- [10] H. Minakata and O. Yasuda, *Phys. Rev. D* **56**, 1692 (1997) [hep-ph/9609276].
- [11] S. M. Bilenky, S. Pascoli and S. T. Petcov, *Phys. Rev. D* **64**, 053010 (2001) [hep-ph/0102265].
- [12] M. Czakon, J. Gluza, J. Studnik and M. Zralek, *Phys. Rev. D* **65**, 053008 (2002) [hep-ph/0110166].
- [13] S. Pascoli, S. T. Petcov and L. Wolfenstein, *Phys. Lett. B* **524**, 319 (2002) [hep-ph/0110287].
- [14] V. Barger, S. L. Glashow, P. Langacker and D. Marfatia, *Phys. Lett. B* **540**, 247 (2002) [hep-ph/0205290].
- [15] H. Nunokawa, W. J. C. Teves and R. Zukanovich Funchal, *Phys. Rev. D* **66**, 093010 (2002) [hep-ph/0206137].
- [16] S. Pascoli, S. T. Petcov and W. Rodejohann, *Phys. Lett. B* **549**, 177 (2002) [hep-ph/0209059].
- [17] F. Deppisch, H. Pas and J. Suhonen, *Phys. Rev. D* **72**, 033012 (2005) [hep-ph/0409306].
- [18] A. Joniec and M. Zralek, *Phys. Rev. D* **73**, 033001 (2006) [hep-ph/0411070].
- [19] S. Pascoli, S. T. Petcov and T. Schwetz, *Nucl. Phys. B* **734**, 24 (2006) [hep-ph/0505226].
- [20] S. Choubey and W. Rodejohann, *Phys. Rev. D* **72**, 033016 (2005) [hep-ph/0506102].
- [21] F. Simkovic, S. M. Bilenky, A. Faessler and T. Gutsche, *Phys. Rev. D* **87**, 073002 (2013) [arXiv:1210.1306 [hep-ph]].
- [22] P. A. R. Ade *et al.* [Planck Collaboration], *Astron. Astrophys.* **571**, A16 (2014) [arXiv:1303.5076 [astro-ph.CO]].
- [23] K. N. Abazajian, E. Calabrese, A. Cooray, F. De Bernardis, S. Dodelson, A. Friedland, G. M. Fuller and S. Hannestad *et al.*, *Astropart. Phys.* **35**, 177 (2011) [arXiv:1103.5083 [astro-ph.CO]].
- [24] R. A. Battye and A. Moss, *Phys. Rev. Lett.* **112**, 051303 (2014) [arXiv:1308.5870 [astro-ph.CO]].
- [25] M. Agostini *et al.* [GERDA Collaboration], *Phys. Rev. Lett.* **111**, 122503 (2013) [arXiv:1307.4720 [nucl-ex]].
- [26] A. Gando *et al.* [KamLAND-Zen Collaboration], *Phys. Rev. Lett.* **110**, 062502 (2013) [arXiv:1211.3863 [hep-ex]].
- [27] J. B. Albert *et al.* [EXO-200 Collaboration], *Nature* **510** 229, (2014) [arXiv:1402.6956 [nucl-ex]].
- [28] M. Auger *et al.* [EXO Collaboration], *Phys. Rev. Lett.* **109**, 032505 (2012) [arXiv:1205.5608 [hep-ex]].
- [29] C. Arnaboldi *et al.* [CUORE Collaboration], *Nucl. Instrum. Meth. A* **518**, 775 (2004) [hep-ex/0212053].

- 
- [30] J. Hartnell [SNO+ Collaboration], J. Phys. Conf. Ser. **375**, 042015 (2012) [arXiv:1201.6169 [physics.ins-det]].
- [31] R. Gaitskell *et al.* [Majorana Collaboration], nucl-ex/0311013.
- [32] R. Arnold *et al.* [SuperNEMO Collaboration], Eur. Phys. J. C **70**, 927 (2010) [arXiv:1005.1241 [hep-ex]].
- [33] V. Alvarez *et al.* [NEXT Collaboration], arXiv:1106.3630 [physics.ins-det].
- [34] J. J. Gomez-Cadenas, J. Martin-Albo, M. Mezzetto, F. Monrabal and M. Sorel, Riv. Nuovo Cim. **35**, 29 (2012) [arXiv:1109.5515 [hep-ex]].
- [35] A. Giuliani and A. Poves, Adv. High Energy Phys. **2012**, 857016 (2012).
- [36] O. Cremonesi and M. Pavan, arXiv:1310.4692 [physics.ins-det].
- [37] V. A. Rodin, A. Faessler, F. Simkovic and P. Vogel, Phys. Rev. C **68**, 044302 (2003) [nucl-th/0305005].
- [38] V. A. Rodin, A. Faessler, F. Simkovic and P. Vogel, Nucl. Phys. A **766**, 107 (2006) [Erratum-ibid. A **793**, 213 (2007)] [arXiv:0706.4304 [nucl-th]].
- [39] E. Caurier, F. Nowacki, A. Poves and J. Retamosa, Phys. Rev. Lett. **77**, 1954 (1996).
- [40] E. Caurier, J. Menendez, F. Nowacki and A. Poves, Phys. Rev. Lett. **100**, 052503 (2008) [arXiv:0709.2137 [nucl-th]].
- [41] F. Simkovic, A. Faessler, H. Muther, V. Rodin and M. Stauf, Phys. Rev. C **79**, 055501 (2009) [arXiv:0902.0331 [nucl-th]].
- [42] M. Kortelainen and J. Suhonen, Phys. Rev. C **75**, 051303 (2007) [arXiv:0705.0469 [nucl-th]].
- [43] M. Kortelainen and J. Suhonen, Phys. Rev. C **76**, 024315 (2007) [arXiv:0708.0115 [nucl-th]].
- [44] J. Barea and F. Iachello, Phys. Rev. C **79**, 044301 (2009).
- [45] J. Barea, J. Kotila and F. Iachello, Phys. Rev. Lett. **109**, 042501 (2012).
- [46] J. Barea, J. Kotila and F. Iachello, Phys. Rev. C **87**, 014315 (2013) [arXiv:1301.4203 [nucl-th]].
- [47] J. Menendez, A. Poves, E. Caurier and F. Nowacki, Nucl. Phys. A **818**, 139 (2009) [arXiv:0801.3760 [nucl-th]].
- [48] A. Gando *et al.* [KamLAND Collaboration], Phys. Rev. D **88**, 033001 (2013) [arXiv:1303.4667 [hep-ex]].
- [49] S. Kettell, J. Ling, X. Qian, M. Yeh, C. Zhang, C. -J. Lin, K. -B. Luk and R. Johnson *et al.*, arXiv:1307.7419 [hep-ex].
- [50] S. -H. Seo, Nucl. Phys. Proc. Suppl. **237**, 65 (2013) See also <http://home.kias.re.kr/MKG/h/reno50>.
- [51] K. Abe *et al.* [T2K Collaboration], Phys. Rev. Lett. **107**, 041801 (2011) [arXiv:1106.2822 [hep-ex]].
- [52] F. P. An *et al.* [Daya Bay Collaboration], Chin. Phys. C **37**, 011001 (2013) [arXiv:1210.6327 [hep-ex]].
- [53] H. Seo, *Recent Results from RENO*, Talk at XXIV Workshop on Weak Interactions and Neutrinos (WIN 2013), September 16-21, Natal, Brazil.
- [54] J. Wolf [KATRIN Collaboration], Nucl. Instrum. Meth. A **623**, 442 (2010) [arXiv:0810.3281 [physics.ins-det]].
- [55] <http://www-ik.fzk.de/katrin/publications/documents/DesignReport2004-12Jan2005.pdf>
- [56] P. A. N. Machado, H. Minakata, H. Nunokawa and R. Zukanovich Funchal, JHEP **1405**, 109 (2014) [arXiv:1307.3248].
- [57] W. Winter, Phys. Rev. D **70**, 033006 (2004) [hep-ph/0310307].
- [58] P. Huber, M. Lindner and W. Winter, JHEP **0505**, 020 (2005) [hep-ph/0412199].
- [59] G. L. Fogli, E. Lisi, A. Marrone, A. Melchiorri, A. Palazzo, P. Serra and J. Silk, Phys. Rev. D **70**, 113003 (2004) [hep-ph/0408045].
- [60] K. A. Olive *et al.* [Particle Data Group Collaboration], Chin. Phys. C **38**, 090001 (2014).
- [61] G. Pantis, F. Simkovic, J. D. Vergados and A. Faessler, Phys. Rev. C **53**, 695 (1996) [nucl-th/9612036].
- [62] J. Kotila and F. Iachello, Phys. Rev. C **85**, 034316 (2012) [arXiv:1209.5722 [nucl-th]].
- [63] S. Riemer-Sorensen, D. Parkinson and T. M. Davis, arXiv:1306.4153 [astro-ph.CO].
- [64] D. Parkinson, S. Riemer-Sorensen, C. Blake, G. B. Poole, T. M. Davis, S. Brough, M. Colless and C. Contreras *et al.*, Phys. Rev. D **86** (2012) 103518 [arXiv:1210.2130 [astro-ph.CO]].
- [65] M. Wyman, D. H. Rudd, R. A. Vanderveld and W. Hu, Phys. Rev. Lett. **112**, 051302 (2014) [arXiv:1307.7715 [astro-ph.CO]].
- [66] J. Hamann and J. Hasenkamp, JCAP **1310**, 044 (2013) [arXiv:1308.3255 [astro-ph.CO]].
- [67] C. Carbone, L. Verde, Y. Wang and A. Cimatti, JCAP **1103**, 030 (2011) [arXiv:1012.2868 [astro-ph.CO]].
- [68] T. D. Kitching, A. F. Heavens, L. Verde, P. Serra and A. Melchiorri, Phys. Rev. D **77**, 103008 (2008) [arXiv:0801.4565 [astro-ph]].
- [69] L. Amendola *et al.* [Euclid Theory Working Group Collaboration], Living Rev. Rel. **16**, 6 (2013) [arXiv:1206.1225 [astro-ph.CO]].
- [70] J. Hamann, S. Hannestad and Y. Y. Y. Wong, JCAP **1211**, 052 (2012) [arXiv:1209.1043 [astro-ph.CO]].
- [71] B. Leistedt, H. V. Peiris and L. Verde, Phys. Rev. Lett. **113**, 041301 (2014) [arXiv:1404.5950 [astro-ph.CO]].
- [72] E. W. Otten and C. Weinheimer, Rept. Prog. Phys. **71** (2008) 086201 [arXiv:0909.2104 [hep-ex]].
- [73] C. Kraus, B. Bornschein, L. Bornschein, J. Bonn, B. Flatt, A. Kovalik, B. Ostrick and E. W. Otten *et*

- 
- al.*, Eur. Phys. J. C **40**, 447 (2005) [hep-ex/0412056].
- [74] V. N. Aseev *et al.* [Troitsk Collaboration], Phys. Rev. D **84**, 112003 (2011) [arXiv:1108.5034 [hep-ex]].
- [75] S. Pascoli and S. T. Petcov, Phys. Lett. B **544**, 239 (2002) [hep-ph/0205022].
- [76] S. Pascoli, S. T. Petcov and W. Rodejohann, Phys. Lett. B **558**, 141 (2003) [hep-ph/0212113].
- [77] S. T. Petcov, New J. Phys. **6**, 109 (2004).
- [78] M. Lindner, A. Merle and W. Rodejohann, Phys. Rev. D **73**, 053005 (2006) [hep-ph/0512143].
- [79] F. Vissani, JHEP **9906**, 022 (1999) [hep-ph/9906525].
- [80] F. Capozzi, G. L. Fogli, E. Lisi, A. Marrone, D. Montanino and A. Palazzo, arXiv:1312.2878 [hep-ph].
- [81] S. R. Elliott and P. Vogel, Ann. Rev. Nucl. Part. Sci. **52**, 115 (2002) [hep-ph/0202264].
- [82] O. Host, O. Lahav, F. B. Abdalla and K. Eitel, Phys. Rev. D **76**, 113005 (2007) [arXiv:0709.1317 [hep-ph]].
- [83] S. Hannestad, arXiv:0710.1952 [hep-ph].
- [84] J. N. Bahcall and C. Pena-Garay, JHEP **0311**, 004 (2003) [hep-ph/0305159].
- [85] H. Minakata, H. Nunokawa, W. J. C. Teves and R. Zukanovich Funchal, Phys. Rev. D **71**, 013005 (2005) [hep-ph/0407326].
- [86] A. Bandyopadhyay, S. Choubey, S. Goswami and S. T. Petcov, Phys. Rev. D **72**, 033013 (2005) [hep-ph/0410283].
- [87] S. -F. Ge, K. Hagiwara, N. Okamura and Y. Takaesu, JHEP **1305**, 131 (2013) [arXiv:1210.8141 [hep-ph]].
- [88] F. Capozzi, E. Lisi and A. Marrone, Phys. Rev. D **89**, 013001 (2014) [arXiv:1309.1638 [hep-ph]].
- [89] H. Minakata, H. Nunokawa and A. A. Quiroga, arXiv:1402.6014v1 [hep-ph].
- [90] F. T. Avignone, G. S. King and Y. .G. Zdesenko, New J. Phys. **7**, 6 (2005).
- [91] F. T. Avignone, III, S. R. Elliott and J. Engel, Rev. Mod. Phys. **80**, 481 (2008) [arXiv:0708.1033 [nucl-ex]].
- [92] M. K. Moe, Nucl. Phys. Proc. Suppl. **19**, 158 (1991).
- [93] S. Dodelson and J. Lykken, arXiv:1403.5173 [astro-ph.CO].